Quantum smectic and supersolid order in helium films and vortex arrays

Leon Balents
Institute for Theoretical Physics, University of California, Santa Barbara, California 93106–4030

David R. Nelson
Lyman Laboratory of Physics, Harvard University, Cambridge, Massachusetts 02138
(Received 15 March 1995)

A flux liquid can condense into a smectic crystal in a pure-layered superconductor with the magnetic field oriented nearly parallel to the layers. Similar order can arise in low-temperature ^{4}He films with a highly anisotropic periodic substrate potential. If the smectic order is commensurate with the layering, this periodic array is *stable* to quenched random pointlike disorder. By tilting and adjusting the magnitude of the applied field, both incommensurate and tilted smectic and crystalline phases are found for vortex arrays. Related variations are possible by changing the chemical potential in the helium system. We discuss transport near the second-order smectic freezing transition, and show that permeation modes in superconductors lead to a small nonzero resistivity and a large but finite tilt modulus in the smectic crystal. In helium films, the theory predicts a nonzero superfluid density and propagating third sound modes, showing that the quantum smectic is always simultaneously crystalline and superfluid.

I. INTRODUCTION

The discovery of high-temperature superconductors, with their broad fluctuation regime, has emphasized the inadequacy of the conventional mean-field description of critical behavior.[1] Early attempts to apply field-theoretic methods to the Ginzburg-Landau (GL) free energy, however, are of limited applicability in low dimensions.[2,3]

Instead, superconducting fluctuations in low dimensions are now understood in terms of vortices, which emerge as the low-energy degrees of freedom of the Ginzburg-Landau theory. The phases of the superconductor within this picture are analogous to states of conventional matter, except that they are composed of flux lines instead of molecules. In fact, because the vortices are extended objects, the system most closely resembles a collection of *quantum* bosons.[4] As the thickness of the superconductor approaches infinity, the effective "temperature" of this bosonic system goes to zero, and interesting strongly correlated phases can emerge.

One difference between the flux-line array and true assemblies of bosons is that in the former, the effects of the embedding medium are more often dramatic. Indeed, without careful preparation, most high-temperature superconducting samples are dominated by internal defects which tend to disorder the vortex array. Only at reasonably high temperatures, when the fluxons are best described as a liquid, can the effects of these random pinning centers be neglected.[5] At lower temperatures, disorder may induce subtle types of glassy order,[6–9] or simply force the system to remain a liquid with very sluggish dynamics.[10]

The layered structure of the copper-oxide materials itself provides a nonrandom source of pinning.[11] At low temperatures, the c-axis coherence length $\xi_{c0} \approx 4$ Å $\lesssim s \approx 12$ Å, where s is the lattice constant in this direction. Vortex lines oriented in the ab plane are attracted to the regions of low condensate electron density between the CuO_2 layers. Such a periodic potential for true two-dimensional bosons could be induced by an anisotropically corrugated substrate, possibly leading to the observation of the effects described here in ^{4}He films.

Previous work on intrinsically pinned vortices has focused on the low-temperature fluctuationless regime, in which the vortices form a pinned elastic solid. Near T_c, however, when thermal fluctuations are important, entirely different phases can exist. These thermally fluctuating states are particularly interesting experimentally because hysteretic effects are weak and equilibrium transport measurements are more easily performed than at low temperatures. Our research is motivated by the recent experimental work of Kwok *et al.*[12] who observed a continuous resistive transition in $YBa_2Cu_3O_7$ for fields very closely aligned ($\theta < 1°$) to the ab plane. A preliminary version of our results appeared in Ref. 13.

To explain the experiments, the interplay between intervortex interactions and thermal fluctuations must be taken into account in an essential way. The experiments of Ref. 12 seem to rule out conventional freezing, which is first order in all known three-dimensional cases. The additional observation of a strong first-order freezing transition for $\theta \gtrsim 1°$ suggests that point disorder is relatively unimportant at these elevated temperatures (strong point disorder would destroy a first-order freezing transition). In addition, an attempted fit of the data to a dynamical scaling form yielded exponents inconsistent with vortex or Bose glass values.[12] Instead, we postulate freezing into an intermediate "smectic" phase between the high-temperature flux liquid and a low-temperature crystal and/or glass. Such smectic freezing, as discussed by de Gennes for the nematic-smectic A transition,[14] can occur via a continuous transition in three dimensions. The vortex smectic state is richer than its liquid crystal counterpart, however, for two reasons. First, the existence of a periodic embedding medium (i.e., the crystal lattice) in the former leads to commensurability effects not present in the liquid crystal.[15] In addition, the connectedness

0163-1829/95/52(17)/12951(18)/$06.00

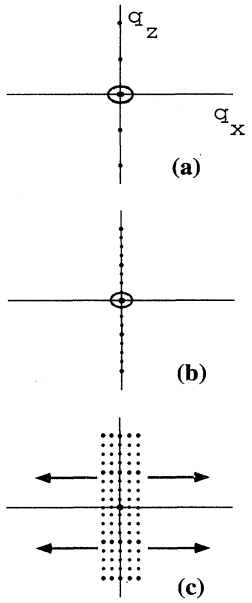

FIG. 1. Schematic structure functions in the (a) liquid, (b) smectic, and (c) solid phases. For simplicity, we have illustrated the case for a square lattice.

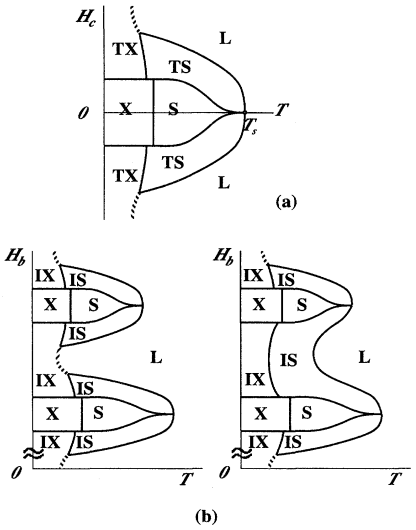

FIG. 2. Phase diagrams in the (a) H_c-T, and (b) H_b-T planes for the disorder-free vortex system. The fuzzy lines indicate first-order transitions. In (b) two possible topologies are shown connecting different commensurate states.

of flux lines leads to constraints with no analog for pointlike molecules. As we show below, the onset of smectic order should be accompanied by a steep drop in the resistivity and a rapid increase in the tilt modulus for fields which attempt to tip vortices out of the CuO_2 planes — see Fig. 10.

The smectic phase may also be distinguished experimentally using neutron scattering, which measures the Fourier transform of the magnetic-field two-point correlation function (see Fig. 1). We assume a magnetic field along the y axis and CuO_2 layers perpendicular to $\hat{\mathbf{z}}$. The vortex liquid structure function shows the usual diffuse liquid rings, as well as δ-function Bragg peaks at $q_z = 2\pi n/s$ (for integral n), representing the "imposed" vortex density oscillations from the CuO_2 layers. On passing to the smectic state, additional peaks develop at wave vectors $q_z = 2\pi n/a$, interlacing between those already present in the liquid. The new peaks represent the broken symmetry associated with preferential occupation of a periodic *subset* of the layers occupied by the vortices in the liquid. At lower temperatures in the vortex solid, further peaks form for $q_x \neq 0$, producing the full reciprocal lattice of a two-dimensional crystal.

Our analysis leads to the phase diagrams shown in Fig. 2. Upon lowering the temperature for $H_c = 0$ and a commensurate value of H_b (here the subscript of H indicates a crystallographic axis), the vortex liquid (L) freezes first at T_s into the pinned smectic (S) state, followed by a second freezing transition at lower temperatures into the true vortex crystal (X). When $H_c \neq 0$, tilted smectic (TS) and crystal (TX) phases appear. The TS-L and TX-L transitions are XY like, while the TS-S and TX-X phase boundaries are commensurate-incommensurate transitions (CIT's).[15] At larger tilts, the TX-TS and TS-L phase boundaries merge into a single first-order melting line. As H_b is changed, incommensurate smectic (IS) and crystal (IX) phases appear, again separated by CIT's from the pinned phases, and an XY transition between the IS and L states. If the low-H_b commensurate smectic (S) phase corresponds to, say, five CuO_2 plane periodicities per vortex layer, the high-H_b S phase will represent a state with four CuO_2 plane periodicities per sheet. We show that the commensurate smectic order along the c axis is *stable* to weak point disorder, in striking contrast to the triangular flux lattice which appears for fields aligned with the c axis.[16] This stability should *increase* the range of smectic behavior relative to the (unstable) crystalline phases when strong point disorder is present.

The high-temperature flux liquid (for fields in the ab plane) is of some interest in its own right. Consider first one vortex line wandering along the y axis, as shown schematically in Fig. 3. This line is subject only to thermal fluctuations and a periodic pinning potential along the z axis, provided by the CuO_2 planes.[17] If thermal fluctuations are

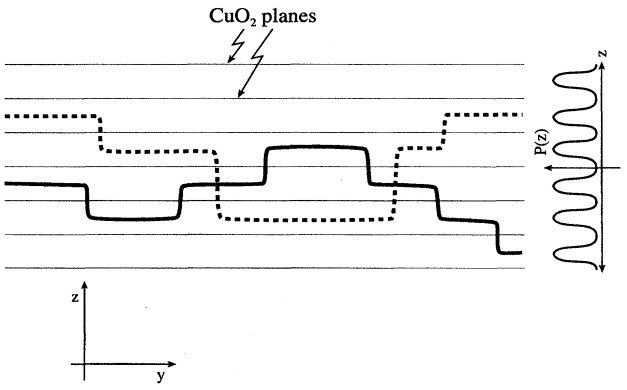

FIG. 3. Wandering of a single flux line (solid curve), leading to an extended probability distribution $P(z)$ given by a $k = 0$ Bloch wave function. Other vortex trajectories (represented by the dashed curve) will generate similar probability distributions, unless interactions lead to crystalline or smectic order.

ignored, the vortex acts like a rigid rod, and will be localized in one of the potential minima.[18] This localization assumption, however, is *always* incorrect in the presence of thermal fluctuations, provided the sample is sufficiently large in the y direction. As $L_y \to \infty$, the statistical mechanics of this single wandering line random walking in directions perpendicular to y leads inevitably to equal probabilities that the vortex is in *any* of the many possible minima along $\hat{\mathbf{z}}$.

On a more formal level, this probability distribution $P(z)$ is given by the square of the ground-state wave function of the Schrödinger equation in a periodic potential — see Sec. III below. The jumps shown in Fig. 3 across CuO_2 planes are represented by quantum-mechanical tunneling in imaginary time. According to Bloch's theorem, this tunneling leads to $P(z)=|\psi_{k=0}(z)|^2$, where the Bloch states in general have the form $\psi_k(z)=\exp(ikz)u(z)$, with $u(z)$ a function with the periodicity of the pinning potential. The resulting probability distribution is shown schematically on the right side of Fig. 3.

Now suppose an additional line is added to the system. As suggested by the trajectory of the dashed curve in Fig. 3, it too will wander from plane to plane. Although the two flux lines interact repulsively, they can wander and still avoid each other by using the x coordinate or by never occupying the same minimum at the same value of the "imaginary time" coordinate y. Thus *both* flux lines generate a delocalized probability distribution and occupy the same $k=0$ Bloch state. At high temperatures or when the lines are dilute, we expect for similar reasons *macroscopic occupation* of the $k=0$ Bloch state in the equivalent boson many-body quantum-mechanics problem, similar to Bose-Einstein condensation. In this sense, the flux liquid is indeed a "superfluid." The presence of numerous "kinks" in the vortex trajectories insures a large tilt response for fields along $\hat{\mathbf{z}}$ and a large resistivity for currents along $\hat{\mathbf{x}}$. The various symmetry-breaking crystalline or smectic states which appear at low temperatures or higher densities arise because of the localizing tendency of the interactions. The density of kinks is greatly reduced in these phases.

The remainder of the paper is organized as follows. In Sec. II, several models are introduced which will be used to analyze the layered superconductor. Sections III and IV discuss the effect of intrinsic pinning on the liquid and crystal phases, respectively, and show how smectic ordering is encouraged on approaching the intermediate regime from these two limits. A Landau theory for the liquid-smectic transition is introduced in Sec. V, and the critical behavior is determined within this model. The nature of the commensurate smectic phase itself is explored in Sec. VI, through a computation of the response functions. In Sec. VII, it is shown to have "supersolid" order, similar to the supersolid crystal phase recently proposed at high magnetic fields along the $\hat{\mathbf{c}}$ axis.[19] The additional phases which arise for large incommensurate fields are described in Sec. VIII. Section IX details the modifications of the phase diagram when weak point disorder is present, and, in particular, demonstrates the stability of the smectic state. Concluding remarks and the implications of these results for helium films on periodically ruled substrates are presented in Sec. X.

II. MODELS

At a fundamental level (within condensed matter physics), layered superconductors may be modeled as a positively charged ionic background and a collection of conduction electrons, which can pair via the exchange of phonons, excitons, magnons, etc. Since such a microscopic theory of high-temperature superconductors is lacking, we must resort to more phenomenological methods. There are, nevertheless, a variety of differing levels of description available, several of which will be used in the remainder of this paper.

A. Static models

The most basic of our models is the familiar Ginzburg-Landau theory, which is an expansion of the free energy of the superconductor in powers of the order-parameter field $\Psi_{\rm GL}$,

$$F_{\rm GL}=F_{\rm SC}+F_{\rm EM},$$

$$F_{\rm SC}=\int d^3\mathbf{r}\left\{\sum_\mu \frac{\hbar^2}{2m_\mu}|D_\mu\Psi_{\rm GL}|^2+\alpha|\Psi_{\rm GL}|^2+\frac{\beta}{2}|\Psi_{\rm GL}|^4\right\},$$

$$F_{\rm EM}=\int d^3\mathbf{r}\frac{1}{8\pi}|\nabla\times\mathbf{A}-\mathbf{H}|^2, \tag{1}$$

where $D_\mu\equiv\partial_\mu-2\pi A_\mu/\phi_0$, $\phi_0=hc/2e$ is the flux quantum. Here $\mathbf{H}$ is the applied external magnetic field. To establish notation, we choose x, y, and z, respectively, along the a, b, and c axes of the underlying cuprate crystal. The diagonal components of the effective mass tensor are then $m_x=m_y\equiv m$ and $m_z=M$. For convenience in what follows, we also define the anisotropy ratio $\gamma\equiv\sqrt{m/M}=\lambda_{ab}/\lambda_c=\xi_c/\xi_{ab}\ll 1$.

Equation (1) provides a powerful means of understanding superconducting behavior, including the effects of anisotropy. In layered materials, however, the theory must be modified to allow for coupling of the superconducting order to the crystalline lattice. One such description, in which the superconductor is regarded as a stack of Josephson-coupled layers, is the Lawrence-Doniach model.[20] For our purposes, however, it is sufficient to consider a "soft" model for the lattice effects, in which the coupling α is allowed to be a periodic function of z with period s equal to the periodicity of the copper-oxide planes.

Because the high-temperature superconductors are strongly type II, it is appropriate to use London theory over a large range of the phase diagram. In this limit, variations of the magnitude of the order parameter are confined to a narrow region within the core of each vortex. Because the resulting London equations are linear, a complete solution can be obtained for the free energy of an arbitrary vortex configuration.[21] For our purposes, it is sufficient to consider an approximate form in which the tilt moduli are local and the interactions between vortices occur at equal y,[22]

$$F_{\rm London}=\sum_i\int dy\,\frac{\tilde{\epsilon}_\parallel}{2}\left|\frac{dx_i(y)}{dy}\right|^2+\frac{\tilde{\epsilon}_\perp}{2}\left|\frac{dz_i(y)}{dy}\right|^2-V_P[z_i(y)]$$
$$+\sum_{i,j}\frac{1}{2}\int dy\,V[\mathbf{r}_{\perp i}(y)-\mathbf{r}_{\perp j}(y)], \tag{2}$$

where $V[\mathbf{r}_\perp] \approx 2\gamma\epsilon_0 K_0(\sqrt{x^2+z^2/\gamma^2}/\lambda_{ab})$ [$K_0(r)$ is a modified Bessel function, $\epsilon_0=(\phi_0/4\pi\lambda_{ab})^2$], and the stiffness constants obtained from anisotropic Ginzburg-Landau (GL) theory are $\tilde{\epsilon}_\parallel=\epsilon_0\gamma$ and $\tilde{\epsilon}_\perp=\epsilon_0/\gamma$ (see, e.g., Ref. 23). $V_P[z]$ is a periodic potential ($V_P[z+s]=V_P[z]$) taking into account the effects of the layering.

Either Eq. (1) or Eq. (2) may be used at finite temperature, by calculating the partition function

$$Z=\mathrm{Tr}e^{-F/k_BT}, \tag{3}$$

where the trace is a functional integral over Ψ_{GL} or the set of vortex trajectories $\{\mathbf{r}_i(z)\}$, for the Ginzburg-Landau and London limits, respectively.

In the London case, this trace may be formally performed by recognizing Eq. (3) as mathematically identical to the Feynmann path integral for the first quantized imaginary time Green's function of interacting bosons. Within this boson analogy,[4] the Green's function may also be calculated using a coherent-state path-integral representation. The "action" for these bosons is

$$\begin{aligned}\tilde{S}_{\mathrm{boson}}=&\int d^3\mathbf{r}\psi^\dagger\left(T\partial_y-\frac{T^2}{2\tilde{\epsilon}_\perp}\partial_z^2-\frac{T^2}{2\tilde{\epsilon}_\parallel}\partial_x^2-\mu\right)\psi\\&-\int d^3\mathbf{r}V_P(z)n(\mathbf{r})\\&+\int d^2\mathbf{r}_\perp d^2\mathbf{r}'_\perp dy\frac{1}{2}V(\mathbf{r}_\perp-\mathbf{r}'_\perp)n(\mathbf{r}_\perp,y)n(\mathbf{r}'_\perp,y),\end{aligned} \tag{4}$$

where ψ is the complex coherent-state boson field, and $n(\mathbf{r})=\psi^\dagger(\mathbf{r})\psi(\mathbf{r})$. It is convenient to rescale $x\to(\tilde{\epsilon}_\perp/\tilde{\epsilon}_\parallel)^{1/2}x$ and $z\to(\tilde{\epsilon}_\parallel/\tilde{\epsilon}_\perp)^{1/2}z$ to obtain the isotropic Laplacian $\nabla_\perp^2\equiv\partial_x^2+\partial_z^2$. Equation (4) becomes

$$\begin{aligned}S_{\mathrm{boson}}=&\int d^3\mathbf{r}\left[\psi^\dagger\left(T\partial_y-\frac{T^2}{2\tilde{\epsilon}}\nabla_\perp^2-\mu\right)\psi-\tilde{V}_P(z)n(\mathbf{r})\right]\\&+\frac{1}{2}\int d^2\mathbf{r}_\perp d^2\mathbf{r}'_\perp dy\tilde{V}(\mathbf{r}_\perp-\mathbf{r}'_\perp)n(\mathbf{r}_\perp,y)n(\mathbf{r}'_\perp,y),\end{aligned} \tag{5}$$

with $\tilde{\epsilon}\equiv\sqrt{\tilde{\epsilon}_\parallel\tilde{\epsilon}_\perp}$ and the rescaled potentials $\tilde{V}_P(z)=V_P(z\gamma^2)$ and $\tilde{V}(\mathbf{r}_\perp)=V(x/\gamma^2,z\gamma^2)$. The action is used via

$$\mathcal{Z}=\int[d\psi^\dagger][d\psi]e^{-S/k_BT} \tag{6}$$

to calculate the grand canonical partition function $\mathcal{Z}$ at chemical potential μ per unit length of vortex line. Equations (6) and (5) may also be obtained directly from a limiting case of Eq. (1) via a duality mapping.[24]

B. Dynamical models

Calculation of dynamical response functions such as the resistivity requires a model for the time dependence of the superconductor. We will do this within the London framework, treating the vortex lines as the dynamical degrees of freedom. In the overdamped limit, the appropriate equation of motion is then

$$\Gamma\dot{\mathbf{r}}_{\perp i}(y)=-\frac{\partial F_{\mathrm{London}}}{\partial\mathbf{r}_{\perp i}(y)}+\mathbf{f}_i, \tag{7}$$

where Γ is a damping constant, and $\mathbf{f}_i$ is the force on the ith flux line, including both external forces and random thermal noise.

Equation (7) is useful in describing the properties of small numbers of vortices. To understand the bulk behavior of dense phases, however, we need an extensive theory. Such a model for the liquid phase was constructed on physical and symmetry grounds in Ref. 25 in the hydrodynamic limit. Because we intend to go beyond simple linearized hydrodynamics, we require some knowledge of the nonlinear form of the bulk equations of motion.

We proceed by first defining the hydrodynamic fields

$$n(\mathbf{r})=\sum_i\delta[\mathbf{r}_\perp-\mathbf{r}_{\perp i}(y)], \tag{8}$$

$$\boldsymbol{\tau}(\mathbf{r})=\sum_i\delta[\mathbf{r}_\perp-\mathbf{r}_{\perp i}(y)]\frac{d\mathbf{r}_{\perp i}(y)}{dy}, \tag{9}$$

$$\mathbf{f}(\mathbf{r})=\sum_i\delta[\mathbf{r}_\perp-\mathbf{r}_{\perp i}(y)]\mathbf{f}_i. \tag{10}$$

Conservation of magnetic flux is embodied in the constraint

$$\partial_y n+\nabla_\perp\cdot\boldsymbol{\tau}=0. \tag{11}$$

Equation (2) may be rewritten as a function of $\mathbf{n}$ and $\boldsymbol{\tau}$, formally

$$F_{\mathrm{London}}[\{\mathbf{r}_{\perp i}(y)\}]=F[n(\mathbf{r}),\boldsymbol{\tau}(\mathbf{r})]. \tag{12}$$

Specific forms for $F[n,\boldsymbol{\tau}]$ will be used as needed.

Equation (7) completely specifies the dynamics of n and $\boldsymbol{\tau}$. Differentiating Eqs. (8) and (9) then leads immediately to hydrodynamic equations of motion. Details are given in Appendix A. One finds

$$\partial_t n+\nabla_\perp\cdot\mathbf{j}_v=0, \tag{13}$$

$$\partial_t\tau_\alpha+\partial_\beta j_{\beta\alpha}=\partial_y j_{v,\alpha}, \tag{14}$$

where the density and tangent currents are

$$\Gamma\mathbf{j}_v=-n\nabla_\perp\frac{\delta F}{\delta n}+n\partial_y\frac{\delta F}{\delta\boldsymbol{\tau}}-\tau_\alpha\nabla_\perp\frac{\delta F}{\delta\tau_\alpha}+n\mathbf{f}, \tag{15}$$

$$\begin{aligned}\Gamma j_{\beta\alpha}=&-\tau^\beta\partial_\alpha\frac{\delta F}{\delta n}+\tau^\beta\partial_y\frac{\delta F}{\delta\tau_\alpha}-\tau^{\beta\gamma}\partial_\alpha\frac{\delta F}{\delta\tau_\gamma}+\tau^\beta f^\alpha\\&-(\beta\leftrightarrow\alpha),\end{aligned} \tag{16}$$

where

$$\tau^{\beta\gamma}(\mathbf{r})\equiv\sum_i\delta[\mathbf{r}_\perp-\mathbf{r}_{\perp i}(y)]\frac{dx_i^\beta}{dy}\frac{dx_i^\gamma}{dy}. \tag{17}$$

Because the constitutive relation for the tangent current includes $\tau^{\beta\gamma}$, Eqs. (13)–(17) do not form a closed set. Vortex hydrodynamics, however, leads us to expect that n and $\boldsymbol{\tau}$ provide a complete long-wavelength description of the sys-

tem. We therefore adopt the truncation scheme $\tau^{\beta\gamma}\rightarrow\langle\tau^{\beta\gamma}\rangle$ (i.e., $\tau^{\beta\gamma}$ is preaveraged at equilibrium). Averaging via Eq. (2) gives

$$\tau^{\beta\gamma}\rightarrow k_BTn\left(\frac{\delta^{\beta x}\delta^{\gamma x}}{\tilde{\epsilon}_{\parallel}}+\frac{\delta^{\beta z}\delta^{\gamma z}}{\tilde{\epsilon}_{\perp}}\right). \tag{18}$$

To complete the dynamical description, we must specify Γ and $\mathbf{f}$. Matching to the liquid hydrodynamics of Ref. 25 relates Γ to the Bardeen-Stephen friction coefficient $\gamma_{\rm BS}=n_0\Gamma$, and gives the driving force

$$\mathbf{f}=\frac{\phi_0}{c}\mathbf{J}\wedge\hat{\mathbf{y}}+\boldsymbol{\eta}. \tag{19}$$

Here $\mathbf{J}$ is the applied transport current density and $\boldsymbol{\eta}(\mathbf{r})$ is a random thermal noise.

III. INTRINSIC PINNING IN THE VORTEX LIQUID

To better understand the interplay of thermal fluctuations and layering of the superconductor, it is useful to first consider the behavior at high temperatures in the liquid state. As discussed by Marchetti,[26] the physics of a single vortex line in the liquid is well described by a hydrodynamic coupling to the motion of other vortices. In the dense limit, this medium is approximately uniform, and does not significantly affect the wandering of an isolated vortex. To estimate the effects of intrinsic pinning, it is thus appropriate to consider a single vortex line, oriented along the a-b plane.

For $T\gtrsim 80$ K, $\xi_c\approx\xi_{c0}(1-T/T_c)^{-1/2}\gtrsim s$. In this limit, the copper-oxide planes act as a smooth periodic potential on the vortex. The magnitude of this potential per unit length is[27]

$$U_p\approx 5\times 10^2\epsilon_0\gamma\left(\frac{\xi_c}{s}\right)^{5/2}e^{-15.8\xi_c/s}. \tag{20}$$

For a single vortex, Eq. (2) reduces to

$$F_v=\int_0^L dy\left\{\frac{\tilde{\epsilon}_{\parallel}}{2}\left|\frac{dx}{dy}\right|^2+\frac{\tilde{\epsilon}_{\perp}}{2}\left|\frac{dz}{dy}\right|^2-V_P(z)\right\}. \tag{21}$$

The periodic potential $V_P[z]=U_pf_p[z/s]$, where $f_p(u)=f_p(u+1)$ is a smooth periodic function with magnitude of order unity.

The x displacement decouples in Eq. (21), and may be integrated out to yield

$$\langle[x(y)-x(0)]^2\rangle\sim D_xy, \tag{22}$$

with $D_x=k_BT/\tilde{\epsilon}_{\parallel}$. The z-dependent part of Eq. (21) is identical to the Euclidean action of a quantum particle of mass $\tilde{\epsilon}_{\perp}$ in a one-dimensional periodic potential $V_P(z)$, with y playing the role of imaginary time. The single flux-line partition function,

$$\mathcal{Z}_1=\int[dz(y)]e^{-F_v[z]/k_BT}, \tag{23}$$

with fixed endpoints, maps to the Euclidean Green's function for the particle, with k_BT replacing $\hbar$.

In the quantum-mechanical analogy, the particle tunnels between adjacent minima of the pinning potential, leading, as discussed in the Introduction, completely delocalized Bloch wave functions even for *extremely* strong pinning. The "time" required for this tunneling maps to the distance $L_{\rm kink}$ in the y direction between kinks in which the vortex jumps across one CuO_2 layer. The WKB approximation gives

$$L_{\rm kink}\sim s\sqrt{\frac{\tilde{\epsilon}_{\perp}}{U_p}}e^{\sqrt{\tilde{\epsilon}_{\perp}U_p}s/k_BT}. \tag{24}$$

Equation (24) may also be obtained from simple scaling considerations. The energy of an optimal kink is found by minimizing

$$f_1\sim\frac{\tilde{\epsilon}_{\perp}}{2}\left(\frac{s}{w}\right)^2w+U_pw \tag{25}$$

over the width (in the y direction) w, giving $w^*\sim\sqrt{\tilde{\epsilon}_{\perp}/U_p}s$ and $f_1^*\sim\sqrt{\tilde{\epsilon}_{\perp}U_p}s$. Such a kink occurs with a probability proportional to $\exp(-f_1^*/k_BT)$ in a length w. The condition $L_{\rm kink}/w\exp(-f_1^*/k_BT)\sim O(1)$ then gives Eq. (24).

When the sample is larger than $L_{\rm kink}$ along the field axis, the flux line will wander as a function of y, with

$$\langle[z(y)-z(0)]^2\rangle\sim D_zy, \tag{26}$$

where the "diffusion constant" $D_z\approx s^2/L_{\rm kink}$.

For $\sqrt{\tilde{\epsilon}_{\perp}U_p}s\lesssim k_BT$, the pinning is extremely weak, and the WKB approximation is no longer valid. Instead, the diffusion constant $D_z\approx k_BT/\tilde{\epsilon}_{\perp}$, as obtained from Eq. (21) with $U_p=0$. At much lower temperatures, when $\xi_c\ll s$, the energy in Eq. (20) must be replaced by the cost of creating a "pancake" vortex[28] between the CuO_2 planes. In this regime, $L_{\rm kink}\sim\xi_{ab}(s/\xi_c)^{\epsilon_0s/k_BT}$.

For $T\approx 90$ K, as in the experiments of Kwok *et al.*[12] $\xi_c/s\approx 2.3$, and Eq. (20) gives $\sqrt{\tilde{\epsilon}_{\perp}U_p}s/k_BT\ll 1$, indicative of weakly pinned vortices in the liquid state. The transverse wandering in this *anisotropic* liquid is described by a boson wave function with support over an elliptical region of area $k_BTL_y/\sqrt{\tilde{\epsilon}_{\parallel}\tilde{\epsilon}_{\perp}}$ with aspect ratio $\Delta x/\Delta z=\gamma^{-1}\approx 5$ for $YBa_2Cu_3O_7$. For $L_y\approx 1$ mm, a typical sample dimension along $\hat{\mathbf{y}}$, the dimensions of this ellipse are of order microns. Since typical vortex spacings at the fields used in Ref. 12 are of order 400 Å, these flux lines are highly entangled.

To understand the bulk properties of the vortex liquid, it is useful to employ the hydrodynamic description of Sec. II B. In the liquid, the appropriate form of the free energy is[25,29]

$$F_L=\frac{1}{2n_0^2}\int\frac{d^3\mathbf{q}}{(2\pi)^3}\{c_{11}(\mathbf{q})|\delta n(\mathbf{q})|^2+c_{44,\parallel}(\mathbf{q})|\tau_x(\mathbf{q})|^2+c_{44,\perp}(\mathbf{q})|\tau_z(\mathbf{q})|^2\}-\int d^3\mathbf{r}V_P[z]\delta n(\mathbf{r}), \tag{27}$$

where $\delta n=n-n_0$, with $n_0=B_y/\phi_0$ the mean density. Here the compression modulus c_{11} and tilt moduli $c_{44,\perp}$ and $c_{44,\parallel}$ are regular functions of $\mathbf{q}$ with finite values at $\mathbf{q}=\mathbf{0}$.

On physical grounds, we expect intrinsic pinning to enter Eq. (27) both through an increase in $c_{44,\perp}$, which decreases fluctuations perpendicular to the layers, and through the $\tilde{V}_P$ term which tends to localize the vortices near the minima in the periodic potential.

The former effect only acts to increase the anisotropy of the liquid. The latter term, however, explicitly breaks translational symmetry along the z axis, inducing a modulation of the vortex density,

$$\int dz e^{-iq_z z}\langle \delta n(\mathbf{r})\rangle = \frac{n_0^2}{c_{11}(q_z, q_x=q_y=0)} V_P[q_z]. \tag{28}$$

This modulation corrects the static structure function, $S(\mathbf{q})=\langle \delta n(\mathbf{q})\,\delta n(-\mathbf{q})\rangle/(2\pi)^3\delta^{(3)}(\mathbf{q}=\mathbf{0})$, according to

$$S(\mathbf{q}) = S_0(\mathbf{q}) + \frac{n_0^4}{[c_{11}(q_z)]^2}|V_P[q_z]|^2(2\pi)^2\delta(q_x)\,\delta(q_y), \tag{29}$$

where $S_0(q)$ is the static structure function for $V_P=0$. Since $V_P[z]$ is a periodic function, the correction term shows peaks at the discrete reciprocal-lattice vectors for which q_z is an integral multiple of $2\pi/s\hat{\mathbf{z}}$.

The situation is somewhat analogous to applying a weak uniform field to a paramagnet, inducing a proportionate magnetization. Unlike the magnetic case, however, the layering perturbation leaves a residual translational symmetry under shifts $z\to z+s$. It is the breaking of this discrete group which we will identify with the freezing of the vortex liquid.

IV. THE CRYSTAL PHASE

Considerable work already exists on intrinsic pinning in vortex crystals.[11] We review the essential ideas here, and discuss its implications for thermal fluctuations at low temperatures.

A. Zero-temperature properties

To study the effect of layering upon the vortex state, we first consider the limit of a weak periodic modulation of the order parameter along the z axis. In this case, the resulting (zero-temperature) configuration is only slightly perturbed from the ideal lattice predicted by Ginzburg-Landau (or London) theory. The free energy in this case may be written in terms of the phonon coordinates $\mathbf{u}(\mathbf{r})$, as

$$F_{\text{elastic}} = \int \frac{d^3\mathbf{q}}{(2\pi)^3}\frac{K_{\alpha\beta ij}}{2} q_\alpha q_\beta u_i(\mathbf{q})u_j(-\mathbf{q}) + F_{\text{IP}}, \tag{30}$$

where i and $j=x,y$, α and $\beta=x,y,z$, and the contribution to the free energy of the layering potential is

$$F_{\text{IP}} = -\int dy \sum_{x_n,z_n} V_P[z_n + u_z(x_n, y, z_n)]. \tag{31}$$

In general the elasticity theory is quite complex due to the anisotropy and wave-vector dependence on the scale of λ. Rather than work with a specific form of the elastic moduli, we will obtain general expressions in terms of an unspecified set of $K_{ij}(\mathbf{q})\equiv K_{\alpha\beta ij}q_\alpha q_\beta$.

To obtain the correct continuum limit of Eq. (31), we consider the possible commensurate states of the layers and vortex array. The triangular equilibrium lattice in this orientation is described by the two lattice vectors $\mathbf{a}_1 = C\gamma^{-1}\hat{\mathbf{z}}$, $\mathbf{a}_2 = C\gamma^{-1}/2(\hat{\mathbf{z}}+\sqrt{3}\gamma^2\hat{\mathbf{x}})$, with $C^2 = 2\phi_0/\sqrt{3}B_y$. Commensurability effects occur when the minimum z displacement between vortices, $C/(2\gamma) = (n/m)s$, where n and m are integers, chosen relatively prime for definiteness. This gives the commensurate fields

$$B_y^{(m,n)} = \frac{m}{n}\frac{\phi_0}{2\sqrt{3}\gamma^2 s^2}. \tag{32}$$

For simplicity we consider here only the integral states with $m=1$. In this case, $V_P[z_n+u]=V_P[u]$, and we can straightforwardly take the continuum limit

$$F_{\text{IP}} = -\int d^3\mathbf{r} V_P[u_z(\mathbf{r})]. \tag{33}$$

Such an expression may be derived explicitly from the Abrikosov solution for fields near H_{c2},[11] in which case the pinning potential is

$$V_P[u] \approx \frac{Hj_c s}{2\pi c}\cos(2\pi u_z/s), \tag{34}$$

where

$$j_c = \frac{4}{\beta_A\sqrt{\pi}}\frac{c(H_{c2}-H)}{\kappa^2 s}\frac{\xi_c\gamma^2}{s}\exp(-8\xi_c^2/s^2). \tag{35}$$

Here $\kappa=\lambda_{ab}/\xi_{ab}$ is the usual Ginzburg-Landau parameter, and $\beta_A\approx 1.16$.

From Eqs. (30) and (33), it is clear that for these commensurate fields, the ground state is unchanged, i.e., $\mathbf{u}=\mathbf{0}$. Away from these fields, however, the fate of the lattice is less obvious. Ivlev *et al.*[11] have shown that, for a small deviation from a commensurate field, it is energetically favorable for the vortex lattice to shear in order to remain commensurate with the copper-oxide plane spacing. Because such a distortion requires some additional free energy, it will generally be favorable, in addition, for the internal magnetic induction $\mathbf{B}$ to deviate from the applied field $\mathbf{H}$ to allow a better fit to the crystal. This Meissner-like effect will be discussed in more detail in Sec. VIII.

For strong layering, such as that described by the Lawrence-Doniach model, the pinning effects are much more pronounced. When $\xi_c \ll s$, the magnetic field remains essentially confined between the CuO_2 layers, and the vortex array is thus *automatically* commensurate at all applied fields. Although such strong confinement of vortices can lead to interesting nonequilibrium states,[30] we will confine our discussion to equilibrium.

B. Thermal fluctuations about the commensurate state

Thermal fluctuations of the vortex lattice are described by the partition function

$$\mathcal{Z}_{\text{elastic}} = \int [du(\mathbf{r})]\exp(-F_{\text{elastic}}/k_B T). \tag{36}$$

In three dimensions, phonon fluctuations are small, and expanding the pinning potential around its minimum for small $\mathbf{u}$, gives the quadratic free energy

$$F_{\text{elastic}} \approx \int \frac{d^3\mathbf{q}}{(2\pi)^3} \frac{K_{ij}(\mathbf{q})}{2} u_i(\mathbf{q}) u_j(-\mathbf{q}) + \frac{\Delta}{2} |u_z(\mathbf{q})|^2, \tag{37}$$

where $\Delta \equiv -V_P''[z=0]$.

The displacement field fluctuations can be calculated from Eq. (37) by equipartition, yielding the general result

$$\frac{\langle u_x^2 \rangle}{k_B T} = \int_{\text{BZ}} \frac{d^3\mathbf{q}}{(2\pi)^3} \frac{K_{zz}(\mathbf{q}) + \Delta}{K_{xx}(\mathbf{q})[K_{zz}(\mathbf{q}) + \Delta] - [K_{xz}(\mathbf{q})]^2}, \tag{38}$$

$$\frac{\langle u_z^2 \rangle}{k_B T} = \int_{\text{BZ}} \frac{d^3\mathbf{q}}{(2\pi)^3} \frac{K_{xx}(\mathbf{q})}{K_{xx}(\mathbf{q})[K_{zz}(\mathbf{q}) + \Delta] - [K_{xz}(\mathbf{q})]^2}, \tag{39}$$

where BZ indicates an integral over the Brillouin zone.

The effect of the periodic potential is thus to uniformly decrease the fluctuations of u_z at all wave vectors. For $\Delta \gtrsim B^2/\lambda^2$, this decrease is substantial over the entire Brillouin zone, and

$$\langle u_x^2 \rangle \approx k_B T \int_{\text{BZ}} \frac{d^3\mathbf{q}}{(2\pi)^3} \frac{1}{K_{xx}(\mathbf{q})}, \tag{40}$$

$$\langle u_z^2 \rangle \approx k_B T \int_{\text{BZ}} \frac{d^3\mathbf{q}}{(2\pi)^3} \frac{1}{\Delta}. \tag{41}$$

In stronger fields, for $\Delta \lesssim B^2/\lambda^2$, only the contributions from $q \lesssim \sqrt{\Delta}/B$ are strongly suppressed. For $1 - B/H_{c2} \ll 1$, Eqs. (34) and (35) can be combined to give the ratio

$$\Delta \lambda^2 / B^2 \approx \frac{2}{\pi^{3/2} \beta_A} (H_{c2}/B - 1) \left(\frac{\xi_c}{s} \right)^3 e^{-8(\xi_c/s)^2}. \tag{42}$$

At lower fields and temperatures, one expects the mean-field estimate above to break down and $\Delta \lambda^2/B^2$ to increase, possibly settling down to a constant value at low temperatures.

For magnetic fields oriented along the c axis, the Lindemann criterion has been used to estimate the melting point of the vortex lattice[4] by requiring that $\langle |\mathbf{u}_i|^2 \rangle = c_L^2 a_i^2$, for $i = x, z$, with a "Lindemann number" $c_L \approx 0.2 - 0.4$. As is clear from Eqs. (38) and (39), once layering is included, the increased stiffness for u_z makes the two ratios $\langle u_x^2 \rangle / a_x^2$ and $\langle u_z^2 \rangle / a_z^2$ unequal. Indeed, the second ratio is strongly suppressed relative to the first. Extending the Lindemann criterion to this situation suggests that the strains in u_x might be alleviated by a partial melting of the lattice without affecting the broken symmetry leading to the u_z displacements. Such a scenario corresponds to the unbinding of dislocations with Burger's vectors along the x axis. The phase in which these dislocations are unbound is the smectic.

C. Strongly layered limit

To further elucidate the nature of the smectic phase, it is helpful to discuss the limit of very strong layering. In this case, the vortex lines are almost completely confined within the spaces between neighboring CuO_2 layers. For moderate fields, occupied layers will be separated by several unoccupied ones, and the interactions between vortices in different layers may be considered weak. Because of the strong layering, the out-of-plane component of the displacement field u_z is suppressed, so that the free energy of the system may be written to a first approximation as

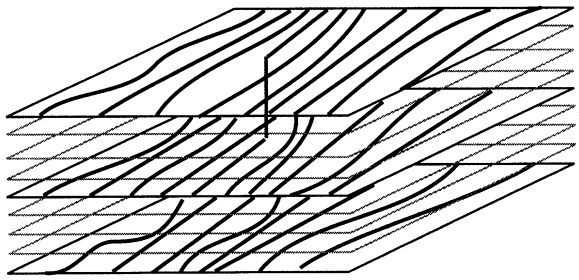

FIG. 4. Hopping of a vortex line between neighboring vortex layers.

$$F_{\text{layers}} = \sum_n \frac{1}{2} \int \frac{d^2\mathbf{q}_\perp}{(2\pi)^2} (K_x q_x^2 + K_z q_z^2) |u_n(\mathbf{q}_\perp)|^2, \tag{43}$$

where $\mathbf{q}_\perp = (q_x, q_y)$ and $u_n(\mathbf{q}_\perp) = u_x(\mathbf{q}_\perp, ns)$. For a qualitative discussion of smectic ordering, it is sufficient to take K_x and K_y independent of $\mathbf{q}$.

Equation (43) neglects both interlayer interactions and hopping. The former are included perturbatively via the free energy

$$F_{\text{int}} = -\sum_n \int dx dy v_{\text{IL}} \cos \frac{2\pi}{a} (u_{n+1} - u_n), \tag{44}$$

where v_{IL} is an interlayer interaction energy and a is the lattice spacing in the x direction. The periodic form of the interaction is required by the symmetry under lattice translations $u \to u + a$ within each layer.

Once hopping of flux lines between neighboring occupied layers is included, u_n is no longer single valued within a given layer. In fact, a configuration in which a single line hops from layer n to layer $n+1$ corresponds to a dislocation in layer n paired with an antidislocation in layer $n+1$, since

$$\oint \nabla u_k \cdot d\ell = a(\delta_{k,n} - \delta_{k,n+1}) \tag{45}$$

for a contour surrounding the hopping point (see Fig. 4). Such dislocation-antidislocation pairs, which we will refer to as large kinks, can be created in neighboring layers with a dislocation fugacity $y_d = \exp(-E_{\text{lk}}/k_B T)$, where the core energy

$$E_{\text{lk}} \approx \sqrt{\tilde{\epsilon}_\perp U_p} ms, \tag{46}$$

as estimated from Eq. (25) with $s \to ms$. Note that the dislocation and antidislocation must have the same x and y coordinates, since misalignment is accompanied by an energy cost proportional to the extra length of vortex between the occupied layers.

The full theory described by Eqs. (43) and (45) plus dislocations can be studied using a perturbative renormalization-group (RG) expansion in v_{IL} and y_d, using techniques developed for the XY model in a symmetry–

breaking field.[31] For $y_d = v_{\rm IL} = 0$, the Gaussian free energy of Eq. (43) describes a fixed line of independently fluctuating vortex layers parameterized by the dimensionless ratio $\sqrt{K_x K_y}/k_B T$. To characterize the order along this fixed line, we define a translational order parameter (characterizing correlations along the x axis) within the nth layer by summing over vortex lines according to

$$\rho_{\|}(x,y,n) \equiv \sum_k \exp[2\pi i x_k^{(n)}(y)/a], \tag{47}$$

where $x_k^{(n)}(y)$ is the coordinate of the kth vortex line in layer n at a length y along the field direction. The correlation function $C_{T,\|}(x,y,n) \equiv \langle \rho_{\|}(x,y,n)\rho_{\|}(0,0,0)\rangle$ is then evaluated by inserting $x_k^{(n)}(y) = ka + u_n(ka,y)$ and converting the sum to an integral via $\Sigma_k \to \int dx/a$. One finds

$$C_{T,\|}(x,y,n) \sim \left(\frac{K}{K_x x^2 + K_y y^2}\right)^{-\pi k_B T/Ka^2} \delta_{n,0}, \tag{48}$$

i.e., quasi-long-range order within the planes.

This fixed line is *always* unstable either to interlayer couplings, to dislocations, or to both perturbations. The linear (in y and $v_{\rm IL}$) RG flows which determine the stability are

$$\frac{dv_{\rm IL}}{dl} = \left(2 - \frac{2\pi k_B T}{Ka^2}\right) v_{\rm IL}, \tag{49}$$

$$\frac{dy_d}{dl} = \left(2 - \frac{Ka^2}{2\pi k_B T}\right) y_d, \tag{50}$$

where $K \equiv \sqrt{K_x K_y}$, and $l = \ln(b/a)$ is the logarithm of the coarse-graining length scale b.

When $k_B T < Ka^2/4\pi$, dislocations are irrelevant at the fixed line, so that y decreases under renormalization. In this regime, however, $v_{\rm IL}$ increases with l, so that interactions between the layers are important for the large distance physics. To study this regime, one may therefore expand the cosine of Eq. (44) in $u_{n+1} - u_n$, obtaining a discrete version of the usual three-dimensional elastic theory. In this limit,

$$C_{T,\|}(x,y,n) \sim \text{const} \tag{51}$$

for large $|x|$, $|y|$, or $|n|$.

At high temperatures, when $k_B T > Ka^2/\pi$, $v_{\rm IL}$ scales to zero, while the fugacity y_d is relevant. Unbound dislocations on long length scales therefore invalidate the elastic theory of Eq. (43). Following standard arguments, the translational correlation function in such an unbound vortex plasma becomes exponentially small, i.e.,

$$C_{T,\|}(x,y,n) \sim \exp(-\tilde{r}/\xi_T), \tag{52}$$

where $\tilde{r} \equiv \sqrt{(K_x/K)x^2 + (K_y/K)y^2 + \chi s^2 n^2}$ with χ a constant, and ξ_T is a finite translational correlation length.

For temperatures in the intermediate range $Ka^2/4\pi < k_B T < Ka^2/\pi$, *both* y_d and $v_{\rm IL}$ are relevant operators. The eventual nature of the ordering at long distances presumably takes one of the two above forms, though the critical boundary at which the system loses long-range translational order in the x direction is not accessible by this method.

It remains to discuss translational order along the layering axis. Such order is characterized by the parameter

$$\rho_{\perp}(x,y,n) \equiv \sum_k \exp(2\pi i z_k^{(n)}(y)/a_z), \tag{53}$$

where a_z is the distance between occupied vortex layers (and therefore an integral multiple of the CuO_2 plane spacing, i.e., $a_z = ms$). Because we have, by construction, confined the vortices to these layers, however, $z_k^{(n)} = na_z$ for every k, and the exponential in Eq. (53) is always unity. Both phases described above, regardless of the relevance of $v_{\rm IL}$ and y, therefore retain long-range order along the z axis.

Within the strongly layered model, there are still excitations which can destroy this transverse ordering. These are configurations in which a flux line hops out of an occupied layer into one of the $(m-1)$ unoccupied intermediate planes between it and the next occupied layer. Such an excursion costs an energy proportional to the length of the vortex segment in the unoccupied layer, so that only short intermediate segments occur at low temperatures. These out-of-plane hops reduce the amplitude $\langle \rho_{\perp} \rangle$, but do not drive it to zero. At very high temperatures, entropy may counterbalance this energy and drive the free energy cost for such intervening vortices negative. Once this occurs, translational order will be lost along the z axis as well, and the system will be a true liquid. Nevertheless, at intermediate temperatures above the unbinding transition for dislocations in the u field but below the temperature at which infinite vortices enter the intermediate copper oxide planes, we expect the system to sustain "one-dimensional" long-range order along the z axis, i.e., a smectic state.

V. CRITICAL BEHAVIOR

Having established the possibility of a smectic phase approaching both from the crystalline and liquid limits, we now focus on the critical behavior near the putative liquid-smectic transition, using a Landau order parameter theory. A closely related Landau theory which describes a low-temperature smectic-crystal transition is discussed in Appendix B. The natural order parameter to describe the smectic ordering is $\rho_{\perp}$ defined in Eq. (53). To simplify notation, we define a new field $\Phi = \rho_{\perp}$, so that, in the continuum notation (i.e., outside the strongly layered limit),

$$n(\mathbf{r}) \approx n_0 \mathrm{Re}\{1 + \Phi(\mathbf{r}) e^{-iqz}\}, \tag{54}$$

where n_0 is the background density, and $q = 2\pi/a_z$ is the wave vector of the smectic layering. The complex translational order parameter $\Phi(\mathbf{r})$ is assumed to vary slowly in space. The superconductor is invariant under translations and inversions in x and y, and has a discrete translational symmetry under $z \to z + s$, where s is the CuO_2 double-layer spacing. From Eq. (54), these periodic translations correspond to the phase shifts $\Phi \to \Phi e^{-iqs}$. We continue to assume, as in the previous section, that $a_z = ms$, with m an arbitrary integer. The most general free energy consistent with these symmetries is

$$F = \int d^3\mathbf{r} \left\{ \frac{K}{2}|(\nabla - i\mathbf{A})\Phi|^2 + \frac{r}{2}|\Phi|^2 + \frac{v}{4}|\Phi|^4 - \frac{g}{2}(\Phi^m + \Phi^{*m}) + \cdots \right\}, \tag{55}$$

where the coordinates have been rescaled to obtain an isotropic gradient term. The "vector potential" $\mathbf{A}$ represents changes in the applied field $\delta\mathbf{H}=\delta H_b\hat{\mathbf{y}}+H_c\hat{\mathbf{z}}$, with $A_x=0$, $A_y=qH_c/H_b$, and $A_z=q\,\delta H_b/H_b$. The form of this coupling follows from the transformation properties of Φ.[14,32]

Equation (55) assumes a *local* form of the free energy. Additional nonlocal interactions arise due to interactions with long-wavelength fluctuations in the density and tangent fields. The most relevant (near the critical point) of these couplings is

$$F_{\Phi-\delta n}=-\gamma\int d^3\mathbf{r}\,\delta n|\Phi|^2, \tag{56}$$

where the correlations of δn are determined from Eqs. (27) and (11).

When $\delta\mathbf{H}=\mathbf{A}=\gamma=0$, Eq. (55) is the free energy of an XY model with an m-fold symmetry-breaking term. A second-order freezing transition occurs within Landau theory when $v>0$ and $r\propto T-T_s$ changes sign from positive (in the liquid) to negative (in the smectic). The renormalization-group (RG) scaling dimension λ_m of the symmetry-breaking term is known *experimentally* in three dimensions to be $\lambda_m\approx 3-0.515m-0.152m(m-1)$.[33] For $m>m_c\approx 3.41$, the field g is irrelevant ($\lambda_m<0$), and the transition is in the XY universality class.[34] The magnetic fields used by Kwok *et al.*[12] correspond to $m=9-11$,[35] well into this regime. The static critical behavior is characterized by the correlation length exponent $\nu\approx 0.671\pm 0.005$ and algebraic decay of order-parameter correlations at T_s,

$$\langle\Phi(\mathbf{r})\Phi^*(\mathbf{0})\rangle\sim\frac{1}{r^{1+\eta}}, \tag{57}$$

with $\eta\approx 0.040\pm 0.003$.[36]

To study the effects of coupling to long-wavelength fluctuations when $\gamma\neq 0$, we first satisfy Eq. (11) by defining an auxiliary "displacementlike" field $\mathbf{w}$ via

$$\delta n=-\nabla_\perp\cdot\mathbf{w},$$

$$\boldsymbol{\tau}=\partial_y\mathbf{w}. \tag{58}$$

After this change of variables, Eq. (27) becomes

$$F_{\mathbf{w}}=\frac{1}{2n_0^2}\int d^3\mathbf{r}\{c_{11}|\nabla_\perp\cdot\mathbf{w}|^2+c_{44,\parallel}|\partial_y w_x|^2+c_{44,\perp}|\partial_y w_z|^2\}, \tag{59}$$

where we have taken the $\mathbf{q}=0$ limits of the elastic moduli to study the critical behavior, and dropped the $V_{\rm IP}$ term which only couples to $\mathbf{w}$ at finite q_z. Equation (56) then becomes

$$F_{\Phi-\mathbf{w}}=\gamma\int d^3\mathbf{r}\nabla_\perp\cdot\mathbf{w}|\Phi|^2. \tag{60}$$

Equation (60) is an anisotropic form of a coupling studied previously in the context of the compressible Ising model, in which $\mathbf{w}$ describes the phonon modes of a compressible lattice on which the spins reside.[37] As shown in Appendix C, the techniques developed for that problem give the renormalization-group eigenvalue $\lambda_\gamma=\alpha/2\nu$ for this coupling at the critical point. Since $\alpha=2-3\nu\approx -0.01$ is negative, the long-wavelength density fluctuations are irrelevant for the critical behavior.

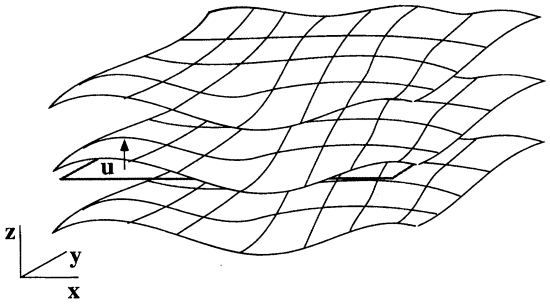

FIG. 5. Fluctuating density wave in the smectic state. Displacements of the layers from their mean positions are described by the field u.

VI. SMECTIC PHASE

A. Static behavior

Deep in the ordered phase ($r<0$), amplitude fluctuations of Φ are frozen out. Writing $\Phi=\sqrt{|r|/v}\,e^{2\pi iu/a}$, Eq. (55) becomes, up to an additive constant,

$$F_{\rm smectic}=\int d^3\mathbf{r}\left\{\frac{\kappa}{2}(\nabla u-\mathscr{A})^2-\tilde{g}\cos 2\pi u/s\right\}, \tag{61}$$

where $a=ms$, $\kappa=4\pi^2|r|K/a^2v$, $\tilde{g}=g(|r|/v)^{m/2}$, and the reduced vector potential is $\mathscr{A}=\mathbf{A}/q$. The displacement field u describes the deviations of the smectic layers from their uniform state (see Fig. 5). The sine-Gordon term is an effective periodic potential acting on these layers. As is well known from the study of the roughening transition,[38] such a perturbation is always relevant in three dimensions. The smectic state is thus *pinned* at long distances (i.e., the displacements u of each smectic layer are localized in a single minima of the cosine).

To further characterize the smectic phase, we consider the transverse magnetic susceptibility, which defines the macroscopic tilt modulus,

$$c_{44,\perp}^{-1}\equiv\left.\frac{\partial B_c}{\partial H_c}\right|_{H_c=0}. \tag{62}$$

The field H_c attempts to tilt the smectic layers. However, $\mathscr{A}\propto H_c$ is an *irrelevant* operator in the smectic phase (as can be easily seen by replacing the periodic potential by a "mass" term $\propto u^2$). This implies that the smectic layers do not tilt under weak applied fields, i.e., $\partial\langle\partial_y u\rangle/\partial H_c|_{H_c=0}=0$. Naively, this implies an infinite tilt modulus.

A more careful treatment shows that $c_{44,\perp}$ actually remains finite in the smectic phase. To compute $c_{44,\perp}$ from first principles, we use the thermodynamic relation

$$B_c=-4\pi\frac{\partial f}{\partial H_c}, \tag{63}$$

where f is the *full* free energy of the system, including a smooth part f_0 not involving Φ and not included in Eq. (55), i.e.,

$$f = f_0 - k_B T \ln \mathcal{Z}_\Phi . \tag{64}$$

To evaluate Eq. (63), we need to consider in detail the dependence of the free energy *and* the coefficients in Eq. (55) on H_c. This dependence arises in two ways, because an applied H_c can be decomposed into a rotation and a scaling of the full field **H**. If the system were fully rotational invariant, the rotational part would enter F purely through the "gauge-invariant" coupling to $\mathcal{A}$ of Eq. (55). However, anisotropy breaks this invariance, leaving instead only an inversion symmetry under $z \to -z$. The inversion symmetry allows for a quadratic dependence of r and of f_0 on H_c.[39] The scaling part also contributes quadratic dependence, which may be combined with the previous effect. Taking both into account, and matching the tilt modulus to the tilt modulus of the liquid phase (i.e., with $\Phi = 0$) leads to

$$B_c = \frac{Kq}{H_b} \mathrm{Im}(\Phi^* \partial_y \Phi) + (c_{44,\perp 0}^{-1} - r''|\Phi|^2) H_c , \tag{65}$$

where $c_{44,\perp 0}$ is the tilt modulus obtained from anisotropic GL theory (without accounting for the discreteness of the layers) and $r'' \equiv \partial^2 r / \partial H_c^2 |_{H_c = 0}$.

Equation (65) has a simple physical interpretation. The first term is the contribution to B_c from tilting of the layers (described by a phase shift of Φ). This term is zero for small fields H_c due to the cosine pinning potential. Even when the layers retain a fixed orientation perpendicular to the c axis, however, the transverse field can penetrate via the second term. Such motion arises microscopically from a nonzero equilibrium concentration of vortices with large kinks extending between neighboring smectic layers, as suggested in Sec. IV C. Equation (65) predicts a nondivergent singularity $c_{44,\perp}(T) - c_{44,\perp}(T_s) \sim |T - T_s|^{1-\alpha}$ at the critical point, where α is the specific-heat exponent.

At low temperatures in the smectic phase, we can estimate the tilt modulus in terms of properties of kinks. In zero field, the concentrations of large kinks carrying magnetic field in the $+\hat{\mathbf{z}}$ and $-\hat{\mathbf{z}}$ directions are equal, leading to zero net field along the c direction. For $H_c \neq 0$, the energy of a kink depends upon its orientation due to the $-B_c H_c / 4\pi$ term in the GL free energy, yielding

$$E_\pm \approx E_{\mathrm{lk}} \pm ms \phi_0 H_c / 4\pi . \tag{66}$$

The difference in the concentrations of up and down kinks takes the activated form

$$n_+ - n_- \sim \frac{B}{\phi_0 w_{\mathrm{lk}}} e^{-E_{\mathrm{lk}}/k_B T} \sinh\left(\frac{ms \phi_0 H_c}{4\pi k_B T} \right), \tag{67}$$

where $w_{\mathrm{lk}} \sim \sqrt{\tilde{\epsilon}_\perp / U_p} ms$, estimated from Eq. (25) with $s \to ms$. Since $B_c = (n_+ - n_-) ms \phi_0$, Eq. (62) yields

$$c_{44,\perp} \approx \left[\frac{\sqrt{\tilde{\epsilon}_\perp / U_p} k_B T}{B \phi_0 ms} \right] e^{E_{\mathrm{lk}}/k_B T}, \tag{68}$$

i.e., a large but finite tilt modulus.

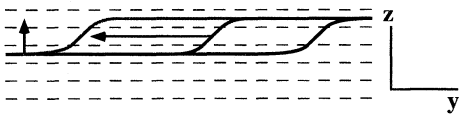

FIG. 6. Sliding of a kink (thick curved line) along the field direction, viewed along the x axis for the case $m = 2$. Dashed lines indicate the copper-oxide layers. As the kink moves along the y axis, net vorticity is transported in the z direction. Such motion produces a finite resistivity in the smectic phase.

B. Dynamical behavior

Very similar phenomena occur in the dynamics of the smectic phase. To study them, we need the equation of motion for Φ. On the basis of symmetry and the lack of obvious conservation laws, a natural conjecture is that of overdamped "model A" (Ref. 40) dynamics. Indeed, a careful treatment using the general formalism of Sec. II B gives (see Appendix D)

$$\gamma_{\mathrm{BS}} \partial_t \Phi = -4q^2 \frac{\delta F_{\mathrm{crit}}}{\delta \Phi^*} + i\mu J_x \Phi - \tilde{\eta}, \tag{69}$$

where $\mu = q \phi_0 n_0 / c$ and $\tilde{\eta}(\mathbf{k}) = i n_0 q \eta_z (q\hat{\mathbf{z}} + \mathbf{k})$. Equation (69) is remarkably similar to the model E dynamics[40] for the complex "superfluid" order parameter Φ, where now J_x plays the role of the "electric field" in the Josephson coupling.[41] The actual electric field is $\mathcal{E}_x = j_{v,z} \phi_0 / c$, leading via Eq. (15) to (see Appendix D)

$$\mathcal{E}_x \approx -\frac{n_0 \phi_0}{2qc} \mathrm{Im}(\Phi^* \partial_t \Phi) + (1 - |\Phi|^2/2) \left(\frac{B}{H_{c2}} \right) \rho_{xx,n} J_x , \tag{70}$$

where $\rho_{xx,n}$ is the normal-state resistivity in the x direction, whose appearance in the last term follows from the relation $(n_0 \phi_0 / c)^2 / \gamma_{\mathrm{BS}} \approx (B/H_{c2}) \rho_{xx,n}$.

Equation (70) is interpreted in close analogy with Eq. (65). In the absence of pinning due to the periodic potential in Eq. (61), an applied force induces a uniform translation of the layers, and thus a net transport of vortices. In the ordered phase, where $\Phi = \sqrt{|r|/v}\, e^{2\pi i u/a}$, the first term in Eq. (70) becomes proportional to the velocity $\partial_t u$. The second term contributes even when the layers are constant. It results microscopically from the motion of equilibrium vortex kinks, which can slide unimpeded along the y axis and thereby transport vorticity along the z axis (see Fig. 6). Such flow at "constant structure" is analogous to the permeation mode in smectic liquid crystals.[14]

The presence of this defective motion implies a small but nonzero resistivity at the L-S transition. Near T_s, Eq. (70) predicts a singular decrease of the form $\rho_{xx}(T) - \rho_{xx}(T_s) \sim |T_s - T|^{1-\alpha}$, similar to the behavior of the tilt modulus. At lower temperatures (but still within the S phase) transport occurs via two channels. The permeation mode gives an exponentially small linear resistivity $\rho_{xx} \sim \exp(-E_{\mathrm{lk}}/k_B T)$ [above T_s, single-layer kinks give $\rho_{xx} \sim \exp(-E_{\mathrm{k}}/k_B T)$, with $E_{\mathrm{k}} \approx E_{\mathrm{lk}}/m$].

Nonlinear transport occurs in parallel to the above linear processes, via thermally activated liberation of vortex droplets, inside which u (or u_z in the crystal phase) is shifted by

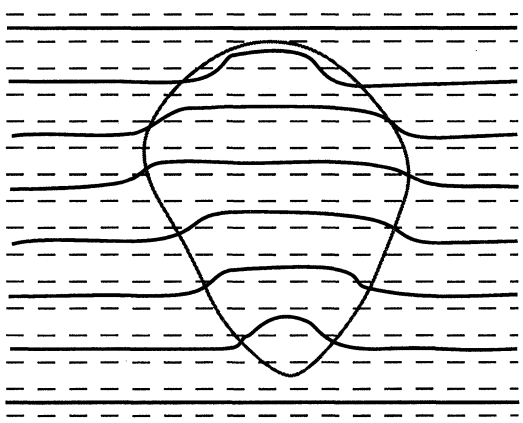

FIG. 7. A two-dimensional cut through a droplet configuration of the smectic layers, drawn for the case $m=2$. The full three-dimensional droplet has a spherical droplet. Inside the droplet (outlined in gray), the layers are shifted by one CuO_2 double layer spacing, $u \to u+s$.

s (see Fig. 7). Such a droplet costs a surface energy, due to the creation of a domain-wall between smectic regions shifted by s. The domain-wall surface tension σ_0 is estimated from

$$\sigma_0 \sim \frac{\kappa}{2}\left(\frac{s}{w}\right)^2 + \tilde{g}w, \tag{71}$$

where w is the width of the domain wall. The first term represents the elastic cost of the shift in u, while the second is the pinning energy. Minimizing Eq. (71) gives $w \sim \sqrt{\kappa/\tilde{g}}s$ and $\sigma_0 \sim \sqrt{\kappa\tilde{g}}s$. This surface energy must be balanced against the Lorentz force in the interior, so that the energy of a droplet of linear size L is

$$E_{\text{droplet}} \sim \sigma_0 L^2 - \frac{JBs}{c}L^3. \tag{72}$$

Equation (72) gives a critical droplet size $L_c \sim \sqrt{\kappa\gamma}c/(JB)$ and an energy barrier $E_B \sim (c/JB)^2(\kappa\gamma)^{3/2}s$. Thermal activation therefore gives

$$\mathscr{E}_{nl} \sim e^{-(J_c/J)^2}, \tag{73}$$

where $J_c \sim (c/B)(\kappa\tilde{g})^{3/4}(s/k_BT)^{1/2}$. Similar nonlinear I-V relations have been obtained previously for vortex and/or Bose glasses,[6,7] but our result is more closely related to surface mobility below the roughening transition on crystal surfaces.[38] Unlike these proposed glass phases, the smectic should always exhibit a nonzero linear resistivity as $\mathbf{J} \to 0$.

VII. SUPERSOLID ORDER AND THE SMECTIC TO CRYSTAL TRANSITION

A. Supersolid nature of the smectic phase

In Secs. VI A and VI B, we have seen that the response functions in the smectic phase retain many of the features of the vortex liquid. Both the tilt modulus and conductivity remain finite, despite the pinning of the smectic density wave by the CuO_2 layers. As discussed earlier, both phenomena are explained by the existence of an equilibrium concentration of large vortex kinks extending between successive occupied vortex layers. These kinks facilitate both transverse magnetic penetration and dissipation for currents along the x axis.

This behavior is strikingly similar to the picture of "supersolid" vortex arrays recently proposed in Ref. 19, for fields parallel to the c axis. In the supersolid, a finite concentration of interstitials or vortices are present in the vortex lattice, and both the tilt modulus and conductivity in the presence of weak pinning are finite. Such a supersolid phase is distinct from the Abrikosov solid in that long-range crystalline order coexists with a finite expectation value of the boson order parameter ψ, i.e.,

$$\langle \psi(\mathbf{r})\psi^*(\mathbf{0})\rangle \to \text{const} \tag{74}$$

as $\mathbf{r} \to \infty$. The supersolid must occur at sufficiently high magnetic fields, but its existence elsewhere in the phase diagram seems unlikely.[19]

Using this characterization of broken $U(1)$ symmetry (under $\psi \to \psi e^{i\theta}$), the vortex smectic is *always* in a supersolid phase. As in Ref. 19, this can be seen by considering the correlation function of ψ's. Note that $\psi(\mathbf{r})$ destroys a vortex line at position $\mathbf{r}$ are $\psi^*(\mathbf{r})$ creates a line in the coherent-state path-integral formalism. Because there is always a finite probability of finding a kink connecting the points $\mathbf{0}$ and $\mathbf{r}$, Eq. (74) is indeed satisfied. With this understanding, the second terms in Eqs. (70) and (65) have an additional complementary interpretation. They correspond to the contributions from the "superfluid fraction" of a two-fluid system with "superfluid" (kink) and "normal" (smectic) parts.

In addition, the concept of symmetry breaking implies that a continuous transition from the flux liquid state (with $\langle\psi\rangle \neq 0$) to a smectic (translationally ordered in one direction) phase must necessarily retain supersolid order. For the smectic phase to appear with $\langle\psi\rangle = 0$ would require *simultaneous* breaking of the discrete translation group and restoration of the $U(1)$ symmetry. Such a double critical point can only occur by tuning two parameters (one in addition to the temperature) or through a first-order transition. The physical arguments of Secs. IV C, VI A, and VI B, of course, imply the stronger condition that the smectic phase must be supersolid at *all* temperatures.

B. Consequences for further transitions at low temperatures

At lower temperatures, provided point disorder remains negligible, the vortices will order along the x axis as well.[42] What is the nature of this two dimensionally ordered phase?

The different possibilities may be classified by the order in which the symmetries are broken. At the lowest temperatures, we expect the system to prefer a true solid phase, with broken translational order in both directions (in particular $\langle\rho_\parallel\rangle \neq 0$, where $\rho_\parallel$ is the amplitude for periodic density variations along the x axis. Recall that $\rho_\perp \equiv \Phi$ is the amplitude for density waves along z) and a restored $U(1)$ symmetry (i.e., no interstitials).[43] To connect this state with the smectic phase in which $\langle\rho_\parallel\rangle = 0$ and $\langle\psi\rangle \neq 0$ requires two changes of symmetry.

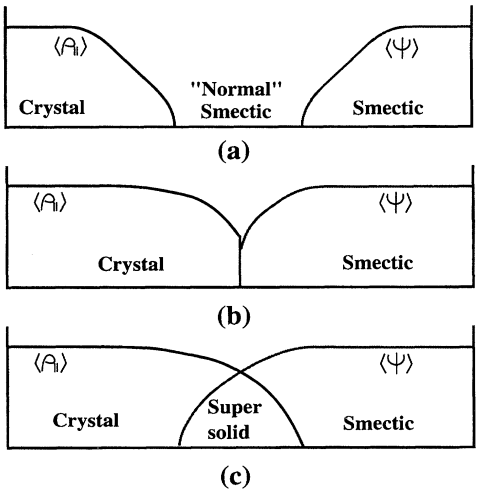

FIG. 8. Three routes of symmetry breaking at low temperatures connecting the smectic phase to the vortex solid. Choice (a) is ruled out on physical grounds. Note that $\langle \rho_\perp \rangle = \langle \Phi \rangle \neq 0$ in all cases.

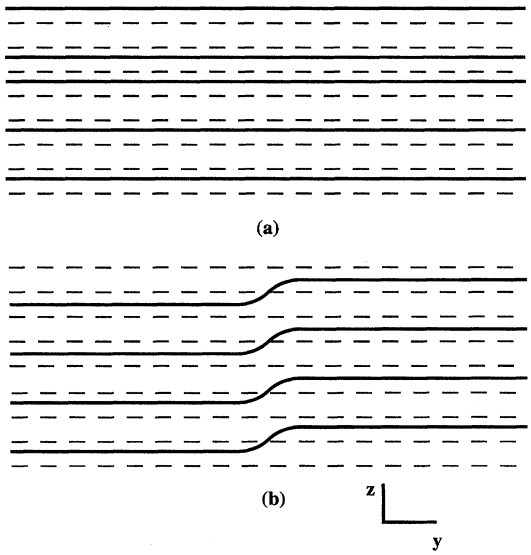

FIG. 9. Kinked configurations (neglecting fluctuations and drawn viewed along the x axis) of the smectic layers for magnetic-field perturbations (a) along the b axis, and (b) along the c axis.

Three monotonic choices of symmetry breaking are shown in Fig. 8. In the scenario (a), upon lowering the temperature from the smectic phase first the $U(1)$ symmetry is restored, and the translational symmetry along the x axis is broken at a lower temperature. As remarked in the previous section, however, the intermediate nonsupersolid smectic phase that appears in this sequence is impossible, so this sequence cannot occur.

Two physical choices remain. The smectic may go directly to the normal solid in a first-order transition which breaks the translational symmetry and restores the $U(1)$ invariance simultaneously, as shown in Fig. 8(b). The last possibility, illustrated in Fig. 8(c), is that of an intermediate supersolid phase between the smectic and the interstitial-free solid. In this case both the low-temperature phase transitions may be second order. The supersolid-solid critical behavior is described in Ref. 19.

The smectic-supersolid transition is once again a freezing transition at a single wave vector, and is potentially describable by a Landau theory like Eq. (55). Because the modulating effect of the underlying crystal lattice is much weaker in the x direction, we expect $g \approx 0$ is a good approximation in this case, which leads to pure XY behavior.

VIII. INCOMMENSURATE PHASES

As is well known from the study of the sine-Gordon model,[15] a large incommensurability can be compensated for by energetically favorable "solitons," or walls across which $u \to u + s$ (see Fig. 9). Solitons begin to proliferate when their field energy per unit area $\sigma_{\rm field} \sim -\kappa \mathscr{A} s$ exceeds their cost at zero field, $\sigma_0 \sim \sqrt{\kappa \tilde{g}} s$ [estimated from Eq. (61)].

Physically, these solitons correspond to extra and/or missing flux-line layers and walls of aligned "jogs" for $\delta \mathbf{H}$ along the b and c axes, respectively (see Fig. 9). In the former case, this leads to an incommensurate smectic (IS) phase, whose periodicity is no longer a simple multiple of s. For $\delta \mathbf{H} \| \hat{\mathbf{z}}$, the solitons induce an additional periodicity along the y axis. This tilted smectic (TS) phase has long-range translational order in two directions.[44] The analogous tilted *crystal* (TX) phase is qualitatively similar, but has long-range order in three directions.

For larger H_c, as the angle between the field and the CuO_2 layers becomes large, intrinsic pinning and anisotropy no longer favor the smectic state. As shown in Fig. 2, we therefore expect the L-TS and TS-TX phase boundaries to merge in this regime. The direct L-TX transition is necessarily first order.

In conventional CIT's, entropic contributions generate additional interactions between domain walls which actually dominate over the bare energetic repulsions when the inter-soliton spacing $\ell \to \infty$. To estimate their magnitude here, we use the well-known logarithmic roughness of a $2d$ interface,[38]

$$\langle (h(\mathbf{x}) - h(\mathbf{0}))^2 \rangle \sim \ln |x|, \tag{75}$$

where h is the height of the interface and the coordinate $\mathbf{x}$ parametrizes its position in the base plane. For solitons spaced by ℓ, collisions between neighbors generally occur only once $h \gtrsim \ell$, so that the size of roughly independently fluctuating regions $x \sim \exp(\ell^2)$. The entropy loss due to this constraint scales with the number of collisions $(L/x)^2$, so that the areal free-energy cost per wall is

$$f_{\rm coll} = -T \Delta s_{\rm coll} \sim T e^{-\ell^2}. \tag{76}$$

Since the energetic interactions in the smectic scale exponentially [like $\exp(-\ell/w)$] at long distances, the collision free energy is actually negligible as $\ell \to \infty$, unlike the situation for lines in $1+1$ dimensions.[15] The free-energy density in the incommensurate phases is thus

$$f_{\rm soliton} \sim -\frac{|\sigma|}{\ell} + \frac{\Delta}{\ell} e^{-l/w}, \tag{77}$$

where $\sigma \equiv \sigma_{\rm field} + \sigma_0 < 0$ is the total areal free energy of the soliton; Δ and w set the energy and length scales of the soliton interactions. At low temperatures we expect $w \sim \lambda$ and $\Delta \sim \epsilon_0 / a_x$, while near T_s, Eq. (61) gives $w \sim \sqrt{\kappa/\tilde{g}s}$ [c.f. Eq. (71)] and $\Delta \sim \tilde{g}\ell$. Minimizing Eq. (77) gives a soliton separation $\ell \sim w \ln(\Delta/|\sigma|)$ near the CIT.

In the TS phase, net vortex motion along the c axis occurs by sliding soliton walls along the b direction. The resulting electric field is proportional to J and the soliton density, leading to an additional contribution to the resistivity which vanishes at the CIT like $\rho_{xx}^{\rm soliton} \sim \rho_0^{\rm soliton}/\ln(\Delta/|\sigma|)$.

A single soliton wall in the IS phase, because it is parallel to the CuO_2 layers, experiences a periodic potential along z. From studies of the roughening transition,[38] it is known that such a periodically pinned wall may be in either a rough or smooth phase. If the walls are individually smooth, thermal fluctuations are negligible, and the assembly of solitons is well described by an effectively one-dimensional elastic chain in a periodic potential.[15] Because they are pinned separately into minima of the potential, they *do not* contribute to ρ_{xx}. If they are rough, they wander logarithmically and eventually interact with their neighbors. The appropriate coarse-grained description beyond this interacting length scale is an elastic stack of domain walls. The configuration of such a stack is described by a second displacement field $u_{\rm dw}$, with a free energy of the same form as Eq. (61) (but with different values of κ and $\tilde{g}$). The statistical mechanics for the $u_{\rm dw}$ field is thus equivalent to that of the original u variable. The preceding analysis must then be repeated within the new effective free energy.

Because of the aforementioned complexity of the one-dimensional problem, we have not attempted to determine the true long-distance behavior of the soliton array in the IS phase. Because the permeation mode in the commensurate smectic already provides a finite tilt modulus and nonzero resistivity, however, we expect that these more subtle effects will have only weak experimental implications.

As the temperature is increased within the IS or TS phases, the system melts into the liquid. To study such transitions, we perform the dilation $\Phi \to \Phi \exp(i\mathbf{A}\cdot\mathbf{r})$. Only the g term is not invariant under such a gaugelike transformation. It becomes oscillatory and therefore does not contribute to the critical behavior at long wavelengths. The IS-L and TS-L phase transitions are thus XY like.

The shape of the CIT phase boundary is of particular experimental interest. In the mean-field regime, this is obtained from the condition $\sigma = 0$ as $\delta H \sim |r|^{\Upsilon}$, with $\Upsilon_{\rm MF} = (m-2)/4$. By the usual Ginzburg criterion, mean-field theory breaks down for $|r| \lesssim (k_B T v / K^{3/2})^2$. To determine the shape of the phase boundary in this critical regime, we follow the RG flows out of the critical region and repeat the preceding analysis with the renormalized couplings determined by matching when $|r|$ is order one. Then $\delta H_R \sim \xi^{\lambda_H} \delta H$ and $g_R \sim \xi^{\lambda_m} g$, with $\xi \sim |r|^{-\nu}$. Rotational invariance at the rescaled fixed point ($g = 0$) implies that the field exponent is *exactly* $\lambda_H = 1$ (see Appendix E). Using these renormalized quantities, we find

$$\Upsilon_{\rm crit} = (|\lambda_m| + 2)\nu/2 \approx 4.9 - 7.2, \tag{78}$$

for the fields used in Ref. 12.

The IS-L and TS-L phase boundaries are nonsingular and are determined locally by the smooth $\delta\mathbf{H}$ dependence of r. In particular, for small H_c, the TS-L phase critical temperature is

$$T(H_c) = T_s - \frac{r''}{2r'} H_c^2, \tag{79}$$

where $r' \equiv \partial r / \partial T|_{T=T_s, \delta H = 0}$.

IX. INFLUENCE OF DISORDER

Lastly, we consider the effects of weak point disorder, which couples to the density of vortices according to

$$F_d = \int d^3\mathbf{r} V_d(\mathbf{r}) n(\mathbf{r}), \tag{80}$$

where $V_d(\mathbf{r})$ is a random potential, which, for point impurities, is short-range correlated in space and narrowly (e.g., Gaussian) distributed at each point. Using Eq. (54), F_d can be rewritten, up to less relevant terms, as

$$F_d = \int d^3\mathbf{r} V_d(\mathbf{r}) \mathrm{Re}\{\Phi(\mathbf{r}) e^{iqz}\}, \tag{81}$$

in the smectic phase and in the liquid sufficiently near T_s. To bring Eq. (81) into a more standard form, we define a complex random field $\tilde{V}_d \equiv V_d e^{iqz}$, in terms of which

$$F_d = \int d^3\mathbf{r} \frac{1}{2} (\tilde{V}_d^* \Phi + \tilde{V}_d \Phi^*). \tag{82}$$

Because of the oscillatory e^{iqz} factor, $\tilde{V}_d$ and $\tilde{V}_d^*$ are essentially uncorrelated at long wavelengths. Equation (82) is the simplest "random-field" XY perturbation of Eq. (55), and the resulting model is known in statistical mechanics as a random-field XY model with an m-fold symmetry-breaking term.

Before discussing the critical behavior of such a theory, it is natural to consider the effect upon the ordered state. In the smectic phase, using $\Phi = \sqrt{|r|/v} \exp(2\pi i u/a)$, Eq. (82) becomes

$$F_d = \int d^3\mathbf{r} \frac{1}{2} \sqrt{\frac{|r|}{v}} (\tilde{V}_d^* e^{2\pi i u/a} + \tilde{V}_d e^{-2\pi i u/a}). \tag{83}$$

If the disorder is weak relative to the periodic potential (i.e., $|\tilde{V}_d| \ll \tilde{g}$), it is naively justified to replace the cosine in Eq. (61) by the "mass" term $(2\pi/s)^2 \tilde{g} u^2/2$. Such a mass term gives a large penalty for excursions of the layers with $u \gtrsim s$, so the randomness in F_d appears irrelevant.

By ignoring the periodicity of the cosine, the above approach does not consider the possibility of disorder-induced solitons. To study the stability of the smectic to such topological defects, consider a region of size L in which the displacement field u is shifted by s, so as not to incur any bulk energy cost from the intrinsic pinning. Within this region, F_d contributes an energy of random sign of order $|V_d| L^{d/2}$ in d dimensions. On the boundary of the region, however, the cosine does contribute, costing an energy $\sim \tilde{g} L^{d-1}$. For $d > 2$, the boundary energy grows more rapidly with L, and the net energy is always positive, provided

$\tilde{g} > |V_d| s^{1-d/2}$. Thus we see that the smectic phase remains *stable* to weak disorder, even once solitons are taken into account.

Note that this result is in strong contrast to the Larkin-Ovchinikov argument that the Abrikosov lattice is unstable to arbitrarily weak pinning.[16] Physically, the instability is prevented, at least for weak disorder, by the periodic pinning potential which increases the stiffness of the smectic displacement field. The result can be understood, however, on more general symmetry grounds. For nonzero g, the system does not have a true continuous translational symmetry in the z direction, but only the discrete symmetry under translations by s. Because the symmetry is discrete, there is no Goldstone mode in the ordered (smectic phase), i.e., phonons are massive. It is now well known that for random-field models with discrete symmetries (e.g., the random-field Ising model, to which our model corresponds when $m=2$), the ordered phase survives above two dimensions.[45] Indeed, the argument given above for stability against droplet solitons is a restatement of the Imry-Ma argument first used for the random-field Ising model.[46]

In the incommensurate (IS and TS) phases, where the periodic pinning $\tilde{g}$ is effectively zero, the Imry-Ma argument no longer applies. In these phases, the original Larkin-Ovchinikov picture holds, and the distortions in $|u(\mathbf{r})|^2$ must grow on long length scales, destroying the long-range translational order of the layers. The nature of the resulting phase is unclear: it may be a "smectic glass," analogous to the proposed vortex-glass phase for more isotropic systems, or it may simply be a strongly correlated liquid, with slow relaxation times. The same considerations hold for the more ordered phases at low temperatures, since the translational order along the x axis lacks the intrinsic pinning required to prevent the Larkin-Ovchinikov instability.

Turning to the critical behavior of the L-S transition, the analysis becomes more subtle. The random-field perturbation in Eq. (82) is a relevant perturbation at the XY fixed point [and indeed at any $O(n)$ fixed point], so the critical behavior is certainly altered. Naively, a $6-\epsilon$ expansion may be made for the critical behavior of the $O(n)$ random-field model, which has a zero-temperature critical point.[47] Within such a perturbative expansion near six dimensions, the symmetry-breaking term appears irrelevant. There are two potential problems with this approach. Firstly, if the symmetry-breaking term indeed remains irrelevant at the new critical point, it would be an example of a three-dimensional random-field XY critical point. The random-field XY model, however, because it has a continuous symmetry, does not even have a stable ordered phase in three dimensions. Although there may not be an obvious contradiction involved in this scenario, the physical meaning is certainly unclear. One possible resolution is that the symmetry-breaking term becomes relevant at some higher dimension (greater than 4). The second problem is the status of the $6-\epsilon$ expansion itself, which has been proven to break down, at least via nonperturbative corrections (but possibly more strongly) for the case of the random-field Ising model.[48] The consistency of the $6-\epsilon$ expansion, even perturbatively, has not yet been determined. Regardless of the success or failure of this theoretical approach, experimental work on random-field Ising systems has demonstrated the subtle types of behavior possible for such zero-temperature critical points. Fortunately, as discussed in Secs. VI A–VII, the supersolid nature of the smectic (with the relatively fast permeation mode) implies that slow dynamics for the smectic ordering will not have a strong impact on transport and magnetization experiments.

Finally, consider the L-IS and L-TS transitions in the presence of disorder. Disorder strongly effects the behavior at such CIT's, because it modifies the wandering of a single domain wall.[49,50] Fortunately, the effects of random field disorder on a single interface are known exactly.[51,52] In contrast to Eq. (75), the height fluctuations of the interface grow like

$$\overline{\langle [h(\mathbf{x})-h(\mathbf{0})]^2 \rangle} \sim |x|^{2\zeta}, \tag{84}$$

where $\zeta=(5-d)/3=2/3$ in three dimensions. Also unlike the pure interface, the free-energy fluctuations within a region grow with length scale, so that the cost per collision scales like $|x|^{\theta}$, where $\theta=d-3+2\zeta=4/3$. The areal collision free energy per wall is thus

$$f_{\rm coll} \sim 1/\ell^{(2-\theta)/\zeta} \sim 1/\ell. \tag{85}$$

This dominates over exponential energetic interactions for large ℓ. The full soliton free energy is thus

$$f_{\rm soliton} \sim -\frac{|\sigma|}{\ell} + \frac{\Delta_d}{\ell^2}, \tag{86}$$

where Δ_d measures the strength of the disorder-induced collision interactions. Minimization of Eq. (86) gives $\ell \sim 1/|\sigma|$.

X. CONCLUSIONS AND APPLICATIONS TO HELIUM FILMS

We have studied the behavior of vortex arrays subjected to a one-dimensional periodic potential transverse to the magnetic field. Such a potential, which is induced by the layered structure of the high-temperature copper-oxide superconductors for fields oriented in the a-b plane, favors an intermediate smectic phase between the vortex lattice and flux liquid. The commensurate smectic state is supersolid, and has in consequence a nonzero finite resistivity and tilt modulus, *despite* being pinned by the periodic potential. Including incommensurability effects leads to the rich phase diagrams of Fig. 2. The experimental signature of the smectic is the appearance of Bragg peaks in the structure function along a single ordering axis interleaving the trivial peaks induced by the layering. We also expect a greatly reduced resistivity for currents transverse to both the layering and magnetic-field axes, and a cusped phase boundary describing the response to small fields perpendicular to the layering direction. The qualitative behavior of the tilt modulus and resistivity near the liquid-to-smectic transition in a field aligned perfectly with the ab plane is shown in Fig. 10.

Using the boson mapping,[4,24] these results can be extended to real two-dimensional quantum-mechanical bosons at zero temperature. The analogous quantum smectic phase might be studied in helium on a periodically ruled substrate. Such a substrate might be approximated by crystalline facets exposing a periodic array of rectangular unit cells with large aspect ratio. There are, however, a number of difficulties

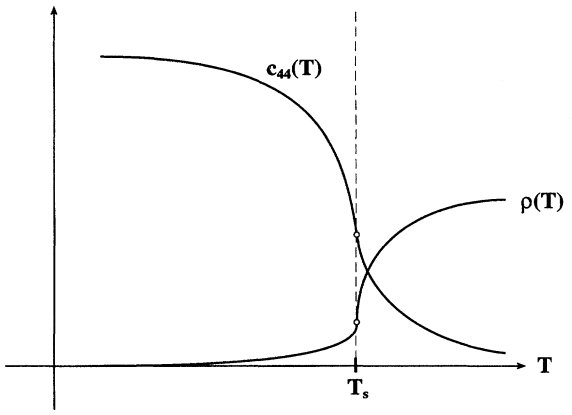

FIG. 10. Tilt modulus and resistivity at T_s for a perfectly aligned commensurate field. Not to scale: the resistivity could appear to drop to zero and the tilt modulus could appear to diverge to infinity in all but the most precise experiments. The open circles denote $|T-T_s|^{1-\alpha}$ singularities, where α is the specific-heat exponent.

inherent in this extension. In particular, the interaction between helium atoms is not purely repulsive; it is reasonably well described by a Lennard-Jones potential with a minimum at an interatomic spacing of a few Angstroms. To obtain a substrate with a small enough period to affect the physics on these length scales is an experimental challenge. Were these interactions purely repulsive, one could probably overcome this difficulty by working with a dilute system. With an attractive tail to the potential, however, a low-density helium film would likely phase separate into helium rich and helium poor regions, making intermediate densities inaccessible. Appropriate experimental conditions may nevertheless be achievable for small values of m (the number of periods of the potential per period of the smectic density wave). The depth of the minimum in the effective pair potential, moreover, could be reduced somewhat by a careful choice of substrate.

The case $m=2$ has been explored numerically in a Bose-Hubbard model in Ref. 53. These authors indeed find a smectic phase, which they denote a "striped solid," with order in reciprocal space at $\mathbf{q}=(\pi,0)$. Their results for the structure function and superfluid density appear to be in good agreement with the predictions of Sec. VI (see in particular their Fig. 11. The superfluid density of the boson system maps onto the inverse tilt modulus c_{44}^{-1} of the flux lines[7]). Unfortunately, a detailed comparison of the critical behavior with the theory is beyond the resolution of the available data.

At a more general level, the liquid-smectic transition treated here appears to be the only known case of continuous quantum freezing in $2+1$ dimensions. The smectic phase, moreover, is perhaps the simplest example of a quantum phase intermediate between solid and liquid. The techniques developed here may be useful in understanding other quantum phases of mixed liquid and/or solid character. One particularly intriguing example is the "Hall solid" proposed in Ref. 54. Through the Chern-Simons mapping,[55] it can be related to a supersolid phase of composite bosons (electrons plus flux tubes).[56] This phase, an analogous "Hall smectic" and "Hall hexatic," and the modifications of the current theory to account for the long-range Coulomb and Chern-Simons interactions are discussed in Ref. 56.

ACKNOWLEDGMENTS

It is a pleasure to acknowledge discussions with George Crabtree, Daniel Fisher, Matthew Fisher, Randall Kamien, Wai Kwok, Leo Radzihovsky, and John Reppy. This research was supported by the National Science Foundation, through Grant No. DMR94-17047 and in part through the MRSEC program via Grant No. DMR4-9400396. L.B.'s work was supported at the Institute for Theoretical Physics by Grant No. PHY89-04035.

APPENDIX A: DERIVATION OF HYDRODYNAMIC EQUATIONS

The continuity equation [Eq. (13)] follows from differentiation of Eqs. (8). For example,

$$\dot{n}=-\sum_i \left[\delta'(x-x_i)\delta(z-z_i)\dot{x}_i+\delta(x-x_i)\delta'(z-z_i)\dot{z}_i\right]$$

$$=-\nabla_\perp\cdot\sum_i \delta(\mathbf{r}_\perp-\mathbf{r}_{\perp i})\dot{\mathbf{r}}_{\perp i}=-\nabla_\perp\cdot\mathbf{j}_v\,, \tag{A1}$$

where

$$\mathbf{j}_v\equiv\sum_i \delta(\mathbf{r}_\perp-\mathbf{r}_{\perp i})\dot{\mathbf{r}}_{\perp i}\,. \tag{A2}$$

Equation (14) is derived analogously, giving the tangent current tensor

$$j_{\beta\alpha}\equiv\sum_i \delta(\mathbf{r}_\perp-\mathbf{r}_{\perp i})\left(\frac{\partial x_i^\beta}{\partial t}\frac{\partial x_i^\alpha}{\partial y}-\frac{\partial x_i^\alpha}{\partial t}\frac{\partial x_i^\beta}{\partial y}\right). \tag{A3}$$

Equations (A2) and (A3) are completely general, and do not depend upon the detailed dynamics of the vortex system. This additional physics is included in the constitutive equations [Eqs. (15) and (16)]. To derive them, we need the equation of motion, Eq. (7). Inserting this into Eq. (A2) gives

$$\Gamma\mathbf{j}_v=-\sum_i \delta(\mathbf{r}_\perp-\mathbf{r}_{\perp i})\frac{\delta F}{\delta\mathbf{r}_{\perp i}(y)}+n\mathbf{f}. \tag{A4}$$

The functional derivative with respect to $\mathbf{r}_{\perp i}$ can be transformed via the chain rule

$$\delta F=\int d^3\mathbf{r}\left[\frac{\delta F}{\delta n(\mathbf{r})}\delta n(\mathbf{r})+\frac{\delta F}{\delta\boldsymbol{\tau}(\mathbf{r})}\cdot\delta\boldsymbol{\tau}(\mathbf{r})\right], \tag{A5}$$

where the variations δn and $\delta\boldsymbol{\tau}$ are

$$\delta n(\mathbf{r})=-\nabla_\perp\cdot\sum_i \delta(\mathbf{r}_\perp-\mathbf{r}_{\perp i})\,\delta\mathbf{r}_{\perp i}(y),$$

$$\delta\boldsymbol{\tau}(\mathbf{r})=-\partial_\alpha\sum_i \delta(\mathbf{r}_\perp-\mathbf{r}_{\perp i})\frac{d\mathbf{r}_{\perp i}}{dy}\delta x_i^\alpha(y)$$

$$+\sum_i \delta(\mathbf{r}_\perp-\mathbf{r}_{\perp i})\frac{d\,\delta\mathbf{r}_{\perp i}}{dy}. \tag{A6}$$

Substituting Eqs. (A5) and (A6) into Eq. (A4) then gives Eq. (15). The constitutive equation for $j_{\beta\alpha}$ is derived analogously, by premultiplying Eq. (7) with $\partial x_i^\beta/\partial y$ and carrying out the same steps as before.

APPENDIX B: LANDAU THEORY OF THE SMECTIC TO CRYSTAL TRANSITION

We assume that $\mathbf{H}$ is in the ab plane and commensurate smectic order is already well established, and ask how a *two*-dimensional vortex modulation then arises at a lower temperature. The modulated vortex density now takes the form

$$n(\mathbf{r})=n_0\mathrm{Re}\{1+\Phi(\mathbf{r})e^{-iqz}+\psi_1(\mathbf{r})e^{-i\mathbf{G_1}\cdot\mathbf{r}}+\psi_2(\mathbf{r})e^{-i\mathbf{G_2}\cdot\mathbf{r}}\}, \tag{B1}$$

where $\Phi(\mathbf{r})$ is the (large) smectic order parameter, and $\mathbf{G}_1$ and $\mathbf{G}_2$ are reciprocal-lattice vectors lying in the $(x$-$z)$ plane with $G_{1x}=-G_{2x}\neq 0$ satisfying

$$q\hat{\mathbf{z}}+\mathbf{G_1}+\mathbf{G_2}=\mathbf{0}. \tag{B2}$$

The six vectors $\pm q\hat{\mathbf{z}}$, $\pm\mathbf{G_1}$, and $\pm\mathbf{G_2}$ form a distorted hexagon of minimal reciprocal-lattice vectors. All other reciprocal-lattice vectors in the crystalline phase are linear combinations of this set, which reflects an anisotropic vortex lattice in real space. The corresponding set of reciprocal-lattice vectors for a *square* lattice is illustrated in Fig. 1.

The complex amplitudes $\psi_1(\mathbf{r})$ and $\psi_2(\mathbf{r})$ are small near the transition, and the Landau free energy difference δF between the smectic and crystalline phases takes the form

$$\delta F=\int d^3\mathbf{r}\left[\frac{\tilde{K}}{2}|\nabla\psi_1|^2+\frac{\tilde{K}}{2}|\nabla\psi_2|^2+\tilde{g}\nabla\psi_1\cdot\nabla\psi_2+\frac{r}{2}(|\psi_1|^2+|\psi_2|^2)+\tilde{w}(\Phi\psi_1\psi_2+\Phi^*\psi_1^*\psi_2^*)+\cdots\right]. \tag{B3}$$

We have equated the coefficients of gradients in all three directions for simplicity. Within mean-field theory, crystalline order can arise via a continuous phase transition whenever $r<0$. The neglected higher-order terms fix the magnitudes of ψ_1 and ψ_2, $|\psi_1|=|\psi_2|\equiv\psi_0$ below the mean-field transition temperature. To study the true transition (which occurs for $r=r_c<0$ due to thermal fluctuations), we set

$$\psi_1=\psi_0e^{i\theta_1(\mathbf{r})},\quad \psi_2=\psi_0e^{i\theta_2(\mathbf{r})}. \tag{B4}$$

Upon neglecting a constant, the free energy becomes

$$\delta F=\int d^3\mathbf{r}\left[\frac{K}{2}|\nabla\theta_1|^2+\frac{K}{2}|\nabla\theta_2|^2+g\nabla\theta_1\cdot\nabla\theta_2+w\cos(\theta_1-\theta_2)\right], \tag{B5}$$

where $K=\tilde{K}\psi_0^2$, $g=\tilde{g}\psi_0^2$, $w=\tilde{w}|\Phi|\psi_0^2$, and we have assumed the phase of the smectic order parameter Φ is locked to zero by the periodic pinning potential. Equation (B5) represents two coupled XY models with phases locked by the cosine. This term forces $\theta_1\approx\theta_2\equiv\theta$, and the phase transition falls in the universality class of a three-dimensional XY model with effective free energy

$$\delta F_{XY}\approx(K+g)\int d^3\mathbf{r}|\nabla\theta|^2. \tag{B6}$$

APPENDIX C: EFFECT OF LONG-WAVELENGTH FLUCTUATIONS AT THE *S*-*L* CRITICAL POINT

To determine λ_γ, we assume the usual scaling form of the free energy at the critical point,

$$f(r,\gamma)=\xi^{-d}g(\gamma\xi^{\lambda_\gamma}), \tag{C1}$$

where g is an unknown scaling function. Using $\xi\sim r^{-\nu}$ and $2-\alpha=d\nu$, Eq. (99) gives

$$\left.\frac{\partial^2 f}{\partial\gamma^2}\right|_{\gamma=0}=\xi^{2\lambda_\gamma-d}g(0)\sim r^{2-\alpha-2\lambda_\gamma\nu}. \tag{C2}$$

The same quantity can be calculated directly, however, by differentiating the partition function to obtain

$$\left.\frac{\partial^2 f}{\partial\gamma^2}\right|_{\gamma=0}=\int d^3\mathbf{x}\langle\nabla_\perp\cdot\mathbf{w}(\mathbf{x})\nabla_\perp\cdot\mathbf{w}(\mathbf{0})\rangle\langle E(\mathbf{x})E(\mathbf{0})\rangle, \tag{C3}$$

where the "energy" operator $E(\mathbf{x})\equiv|\Phi(\mathbf{x})|^2$. The angular brackets indicate expectation values in the decoupled theories. The energy-energy correlations take the scaling form

$$\langle E(\mathbf{x})E(\mathbf{0})\rangle\sim r^{2(1-\alpha)}h(|\mathbf{x}|/\xi), \tag{C4}$$

where $h(\chi)$ is another unknown scaling function. The long-wavelength fluctuations, determined from Eq. (59), are

$$\langle\nabla_\perp\cdot\mathbf{w}(\mathbf{x})\nabla_\perp\cdot\mathbf{w}(\mathbf{0})\rangle=n_0^2k_BT\int\frac{d^3\mathbf{q}}{(2\pi)^3}\frac{c_{44,\perp}q_x^2+c_{44,\parallel}q_z^2}{c_{11}(c_{44,\perp}q_x^2+c_{44,\parallel}q_z^2)+c_{44,\perp}c_{44,\parallel}q_y^2}e^{i\mathbf{q}\cdot\mathbf{x}}. \tag{C5}$$

Inserting Eqs. (C4) and (C5) into Eq. (C3) and changing variables $\mathbf{x}\rightarrow\xi\mathbf{x}$ gives the scaling

$$\left.\frac{\partial^2 f}{\partial\gamma^2}\right|_{\gamma=0}\sim r^{2(1-\alpha)}. \tag{C6}$$

Comparison with Eq. (C2) then gives the desired result $\lambda_\gamma=\alpha/2\nu$.

APPENDIX D: EQUATIONS OF CRITICAL DYNAMICS

To derive the critical equations of motion, we assume that important fluctuations occur only near $\mathbf{q}=\mathbf{0}$ and $\mathbf{q}=q\hat{\mathbf{z}}$. Including the $\mathbf{q}=\mathbf{0}$ modes in Eq. (54) gives

$$n(\mathbf{r})=n_0[1+\mathrm{Re}\Phi e^{-iqz}]+\delta n. \tag{D1}$$

It is sufficient to keep only the small $\mathbf{q}$ parts of the tangent field.[57] The finite q_z modulation of the density induces a modulation of the vortex current,

$$\mathbf{j}_v=\mathbf{j}_{v,u}+\mathrm{Re}\mathbf{j}_{v,s}e^{-iqz}, \tag{D2}$$

where $\mathbf{j}_{v,u}$ and $\mathbf{j}_{v,s}$ are the (slowly varying) uniform and smectic (i.e., periodic) components of the vortex current. Inserting Eq. (D1) into Eq. (15) and isolating the parts proportional to e^{-iqz} gives

$$\Gamma\mathbf{j}_{v,s}=-4\left(1+\frac{\delta n}{n_0}\right)(\nabla_\perp-iq\hat{\mathbf{z}})\frac{\delta F}{\delta\Phi^*}-n_0\Phi\nabla_\perp\frac{\delta F}{\delta(\delta n)}$$
$$+n_0\Phi\partial_y\frac{\delta F}{\delta\boldsymbol{\tau}}+n_0\Phi\mathbf{f}+n_0\mathbf{f}_{\mathrm{thermal}}e^{iqz}, \tag{D3}$$

where the last term is included because the white noise $\mathbf{f}_{\mathrm{thermal}}$ has Fourier components at all wave vectors. Similarly, from the uniform component, one finds

$$\Gamma\mathbf{j}_{v,u}=-(n_0+\delta n)\left[\nabla_\perp\frac{\delta F}{\delta(\delta n)}-\partial_y\frac{\delta F}{\delta\boldsymbol{\tau}}\right]-\tau_\alpha\nabla_\perp\frac{\delta F}{\delta\tau_\alpha}$$
$$-2\mathrm{Re}\left[\Phi(\nabla_\perp+iq\hat{\mathbf{z}})\frac{\delta F}{\delta\Phi}\right]+(n_0+\delta n)\mathbf{f}. \tag{D4}$$

Using Eqs. (D2), the divergence of the current is

$$\nabla_\perp\cdot\mathbf{j}_v=\nabla_\perp\cdot\mathbf{j}_{v,u}+\mathrm{Re}(\nabla_\perp-iq\hat{\mathbf{z}})\mathbf{j}_{v,s}e^{-iqz}, \tag{D5}$$

which leads to the two continuity equations

$$\partial_t\delta n+\nabla_\perp\cdot\mathbf{j}_{v,u}=0, \tag{D6}$$

$$n_0\partial_t\Phi+(\nabla_\perp-iq\hat{\mathbf{z}})\cdot\mathbf{j}_{v,s}=0. \tag{D7}$$

Equations (D3)–(D7) completely specify the dynamics of the density fluctuations δn and Φ. Inserting Eq. (D3) into Eq. (D7), and neglecting irrelevant couplings gives the "model E"-like model of Eq. (69).

Equation (D4) can, in principle, be used to study the effects of the smectic ordering on the long-wavelength modes. The most physical application, however, is to determine the contribution of the smectic degrees of freedom to the electric field. The average bulk (i.e., $\mathbf{q}=\mathbf{0}$) field is $\langle\mathscr{E}_x\rangle=\langle j_{v,u,z}\rangle\phi_0/c$. In the spirit of the Landau expansion, $\mathbf{q}=\mathbf{0}$ component of Eq. (D4) can be reasonably approximated by dropping terms with gradients of Φ (the leading contributions from the first term involving δn and $\boldsymbol{\tau}$ vanished automatically at $\mathbf{q}=\mathbf{0}$ even without this approximation), yielding

$$\Gamma\langle\mathscr{E}_c\rangle\approx n_0\phi_0 f_z/c+\frac{iq\phi_0}{c}\left[\Phi^*\frac{\delta F}{\delta\Phi^*}-\Phi\frac{\delta F}{\delta\Phi}\right]. \tag{D8}$$

Recognizing the variation of the free energy on the right-hand side of Eq. (D8), the substitution [c.f. Eq. (69)]

$$\frac{\delta F}{\delta\Phi^*}=-\frac{\gamma_{\mathrm{BS}}}{4q^2}\partial_t\Phi+\frac{i\mu J_x}{4q^2}\Phi, \tag{D9}$$

leads immediately to Eq. (70).

APPENDIX E: EIGENVALUE OF A

The eigenvalue λ_H is determined completely by rotational invariance. To see this, consider Eq. (55) at the fixed point, i.e., with $g=0$. By making the transformation $\Phi\rightarrow\Phi\exp(i\mathbf{A}\cdot\mathbf{r})$, the term involving $\mathbf{A}$ may be completely removed from F. The free energy is thus independent of $\mathbf{A}$. After integrating out short-wavelength modes, no dependence on $\mathbf{A}$ can appear, so precisely the same transformation must eliminate the field dependence in the renormalized free energy. This operation is $\Phi\rightarrow\Phi\exp(i\mathbf{A}\cdot\mathbf{r}\xi)$, using the rescaled $\mathbf{r}$, so the renormalized vector potential must be

$$\mathbf{A}_R=\xi\mathbf{A}, \tag{E1}$$

which implies $\lambda_H=1$.

[1] Some recent experiments which demonstrate these strong fluctuation effects in clean samples include H. Safar, P. L. Gammel, D. A. Huse, D. J. Bishop, J. P. Rice, and D. M. Ginsberg, Phys. Rev. Lett. **69**, 824 (1992); W. K. Kwok *et al.*, *ibid.* **72**, 1092 (1994).

[2] B. I. Halperin, T. C. Lubensky, and S.-K. Ma, Phys. Rev. Lett. **32**, 292 (1974).

[3] E. Brezin, D. R. Nelson, and A. Thiaville, Phys. Rev. B **31**, 7124 (1985).

[4] D. R. Nelson, Phys. Rev. Lett. **60**, 1415 (1988); D. R. Nelson and S. Seung, Phys. Rev. B **39**, 9153 (1989).

[5] D. R. Nelson and P. Le Doussal, Phys. Rev. B **42**, 10 113 (1990).

[6] D. S. Fisher, M. P. A. Fisher, and D. A. Huse, Phys. Rev. B **43**, 130 (1991).

[7] D. R. Nelson and V. M. Vinokur, Phys. Rev. B **48**, 13 060 (1993).

[8] R. H. Koch, V. Foglietti, W. J. Gallagher, G. Koren, A. Gupta, and M. P. A. Fisher, Phys. Rev. Lett. **63**, 1511 (1989); P. L. Gammel, L. F. Schneemener, and D. J. Bishop, *ibid.* **66**, 953 (1991).

[9] L. Civale, A. D. Marwick, T. K. Worthington, M. A. Kirk, J. R. Thompson, L. Krusin-Elbaum, Y. Sum, J. R. Clem, and F. Holtzberg, Phys. Rev. Lett. **67**, 648 (1991); M. Leghissa, L. A. Gurevich, M. Kraus, G. Saemann-Ischenko, and L. Ya. Vinnikov, Phys. Rev. B **48**, 1341 (1993).

[10] H. S. Bokil and A. P. Young, Phys. Rev. Lett. **74**, 3021 (1995).

[11] B. I. Ivlev and N. B. Kopnin, J. Low Temp. Phys. **80**, 161 (1990); B. I. Ivlev, N. B. Kopnin, and V. L. Pokrovsky, *ibid.* **80**, 187 (1990).
[12] W. K. Kwok, J. Fendrich, U. Welp, S. Fleshler, J. Downey, and G. W. Crabtree, Phys. Rev. Lett. **72**, 1088 (1994).
[13] L. Balents and D. R. Nelson, Phys. Rev. Lett. **73**, 2618 (1994).
[14] P. G. de Gennes and J. Prost, *The Physics of Liquid Crystals* (Oxford University Press, New York, 1993).
[15] J. Villain, in *Ordering in Strongly Fluctuating Condensed Matter Systems*, edited by T. Riste (Plenum, New York, 1980), p. 221.
[16] A. I. Larkin and Yu.-N. Ovchinikov, J. Low Temp. Phys. **34**, 409 (1979).
[17] In real cuprate materials, there is usually more than one such plane per unit-cell spacing in the z direction. In this paper, we will usually ignore such complications, and model the potential by a simple sinusoidal variation along z.
[18] The line is of course still delocalized along the x direction, not shown in the figure.
[19] E. Frey, D. R. Nelson, and D. S. Fisher, Phys. Rev. B **49**, 9723 (1994).
[20] W. E. Lawrence and S. Doniach, in *Proceedings of the 12th International Conference on Low Temperature Physics*, edited by by E. Kanda (Academic Press of Japan, Kyoto, 1971), p. 361.
[21] See, e.g., A. Sudbo and E. H. Brandt, Phys. Rev. Lett. **66**, 1781 (1991), and references therein.
[22] Both the equal-y interaction and the wave-vector-independent elastic moduli are appropriate in situations when the curvature of the vortex lines is small on the scale of λ. See Appendix B of Ref. 7.
[23] G. Blatter, V. B. Geshkenbein, and A. I. Larkin, Phys. Rev. Lett. **68**, 875 (1992).
[24] M. P. A. Fisher and D.-H. Lee, Phys. Rev. B **39**, 2756 (1989).
[25] M. C. Marchetti and D. R. Nelson, Physica C **174**, 40 (1991); Phys. Rev. B **42**, 9938 (1990).
[26] M. C. Marchetti, Phys. Rev. B **43**, 8012 (1991).
[27] A. Barone, A. I. Larkin, and Yu. N. Ovchinnikov, J. Supercond. **3**, 155 (1990).
[28] J. R. Clem, Phys. Rev. B **43**, 7837 (1991).
[29] The static equilibrium hydrodynamic equations described here have been derived from the boson mapping in Ref. 58.
[30] L. S. Levitov, Phys. Rev. Lett. **66**, 224 (1991).
[31] J. V. José, L. P. Kadanoff, S. Kirkpatrick, and D. R. Nelson, Phys. Rev. B **16**, 1217 (1977).
[32] The dilation $z \rightarrow (1+\delta H_b/H_b)z$ leads [cf. Eq. (54)] to $\Phi \rightarrow \Phi e^{iq(\delta H_b/H_b)z}$, since the density n is a scalar. Likewise, the rotation $\mathbf{r} \rightarrow \mathbf{r} + (H_c/H_b)\hat{\mathbf{x}} \wedge \mathbf{r}$ induces $\Phi \rightarrow \Phi e^{iq(H_c/H_b)y}$.
[33] A. Aharony *et al.*, Phys. Rev. Lett. **57**, 1012 (1986). This empirical relation breaks down for very large m.
[34] For $m < m_c$, symmetry-breaking terms are *relevant*, and change the universality class of the transition. The cases $m=2$ and $m=3$ correspond to Ising and three-state Potts models, respectively.
[35] See, e.g., L. J. Campbell, M. M. Doria, and V. G. Kogan, Phys. Rev. B **38**, 2439 (1988).
[36] J. Zinn-Justin, *Quantum Field Theory and Critical Phenomena* (Oxford University Press, New York, 1990), p. 619.
[37] D. J. Bergman and B. I. Halperin, Phys. Rev. B **13**, 2145 (1976).
[38] J. D. Weeks, in *Ordering in Strongly Fluctuating Condensed Matter Systems,* edited by T. Riste (Plenum, New York, 1980), p. 293.
[39] In fact, K and v and other higher-order coefficients also depend on H_c. Their contributions to $c_{44,\perp}$, are, however, small in the limit considered.
[40] P. C. Hohenberg and B. I. Halperin, Rev. Mod. Phys. **49**, 435 (1977).
[41] Our problem differs from model E in that the "conserved density" δn is intimately connected via Eq. (11) to the tangent field τ.
[42] More complex structures are possible. See D. Feinberg and A. M. Ettouhami, Phys. Scr. **T49**, 159 (1993).
[43] It may seem surprising that the $U(1)$ symmetry is unbroken at zero temperature. In the language of statistical mechanics, this is because ψ is actually a *disorder* operator, as can be seen by the duality relation with the original Ginzburg-Landau order parameter Ψ_{GL} (Ref. 24).
[44] Since the solitons are two-dimensional objects embedded in three dimensions, dislocations cannot occur without terminating the wall itself, which is presumably energetically very costly. A dislocation-free stack of layers in three dimensions automatically has long-range order, justifying the description as a crystalline phase.
[45] J. Z. Imbrie, Phys. Rev. Lett. **53**, 1747 (1984).
[46] Y. Imry and S.-K. Ma, Phys. Rev. Lett. **35**, 1399 (1975).
[47] See, e.g., D. Boyanovsky and J. L. Cardy, Phys. Rev. B **27**, 4447 (1983), and D. S. Fisher, Phys. Rev. Lett. **56**, 416 (1986).
[48] See, e.g., D. S. Fisher, Phys. Rev. B **31**, 7233 (1985).
[49] M. Kardar and D. R. Nelson, Phys. Rev. Lett. **55**, 1157 (1985).
[50] T. Nattermann and R. Lipowsky, Phys. Rev. Lett. **61**, 2508 (1988).
[51] G. Grinstein and S.-K. Ma, Phys. Rev. B **28**, 2588 (1983).
[52] L. Balents and D. S. Fisher, Phys. Rev. B **48**, 5949 (1993).
[53] G. G. Batrouni, R. T. Scalettar, G. T. Zimanyi, and A. P. Kampf, Phys. Rev. Lett. **74**, 2527 (1995); R. T. Scalettar, G. G. Batrouni, A. P. Kampf, and G. T. Zimanyi, Phys. Rev. B **51**, 8467 (1995).
[54] Z. Tesanovic, F. Axel, and B. I. Halperin, Phys. Rev. B **39**, 8525 (1989).
[55] See, e.g., S. C. Zhang, Int. J. Mod. Phys. B **6**, 25 (1992).
[56] L. Balents (unpublished).
[57] L. Balents and D. R. Nelson (unpublished).
[58] R. D. Kamien, P. Le. Doussal, and D. R. Nelson, Phys. Rev. A **45**, 8727 (1992).